



Leveraging the Dynamic in Vitro Hollow Fiber Infection Model in Determining Optimal Clinical Dose of β -Lactam and β -Lactamase Inhibitor Combinations.

Citation

Tanudra, Maria. 2018. Leveraging the Dynamic in Vitro Hollow Fiber Infection Model in Determining Optimal Clinical Dose of β -Lactam and β -Lactamase Inhibitor Combinations.. Master's thesis, Harvard Extension School.

Permanent link

<http://nrs.harvard.edu/urn-3:HUL.InstRepos:42004045>

Terms of Use

This article was downloaded from Harvard University's DASH repository, and is made available under the terms and conditions applicable to Other Posted Material, as set forth at <http://nrs.harvard.edu/urn-3:HUL.InstRepos:dash.current.terms-of-use#LAA>

Share Your Story

The Harvard community has made this article openly available.
Please share how this access benefits you. [Submit a story](#).

[Accessibility](#)

Leveraging the Dynamic *in vitro* Hollow Fiber Infection Model in Determining the Optimal
Clinical Dose of β -lactam and β -lactamase Inhibitor Combinations

Maria Angela Tanudra

A Thesis in the Field of Biotechnology
for the Degree of Master of Liberal Arts in Extension Studies

Harvard University

November 2018

Abstract

Infectious disease is one of the top ten leading causes of death worldwide (WHO, 2017). Emergence of new mechanisms of antibiotic resistance continually rises and spreads globally, becoming one of the major global health threats. Without new antibiotics being successfully developed, we are getting closer to a post-antibiotic era where a simple cut can become life-threatening. Significant amounts of time and money are invested on these new drug candidates, however, very few make it to the market, often due to poor PK/PD properties recognized after the failure of lengthy, expensive clinical testing. The aim of this study is to help assess the use of a dynamic *in vitro* PK/PD system, to help predict successful clinical dose, PK/PD target and regimen that would help reduce the development of resistance. *In vitro* and *in vivo* PK/PD models have previously been utilized to help characterize potential drug candidates and their PK/PD properties that would help streamline drug development in its early stages or preventing them from entering development in the first place (Meihbom 2002). The hollow fiber system is a robust *in vitro* PK/PD model that has a potential in helping predict proper clinical doses. The system can be useful in identifying the drug exposure and dosing frequency that will result in an improved therapeutic outcome.

Dedication

To: My husband and sons.

Acknowledgments

To Ed Buurman, thank you for taking the time (and patience) to help me with this thesis. It hasn't been an easy road for me but your encouragement and "nudges" helped me pull through.

John O'Donnell, thank you for being my mentor at AstraZeneca and Entasis and for allowing me to grow as a scientist and allowing me to expand my knowledge and expertise in the PK/PD field.

Renu Singh and Joe Newman, thank you for the Emax modeling data for ATM-AVI and ETX2514Sul. Thank you to AstraZeneca and Entasis for funding all the research.

To my parents for encouraging me to work hard in reaching my goals

To my husband who never gave up on me and encouraged me (with a slight nagging) to finish my work. For giving me all the time and space, I needed to finish my thesis and for being patient with me as I go through personal and professional difficulties. Thank you for being my strength through those moments.

To my sons, this is for you.

Table of Contents

Dedication	iv
Acknowledgments.....	v
List of Tables	viii
List of Figures	ix
Chapter I. Introduction.....	1
Chapter II. Materials and Methods	12
Antimicrobials Agents	12
Bacterial isolates	12
Characterization of isolates through susceptibility testing	13
Dose Response and Dose Fractionation Study Design	14
Hollow Fiber system set-up	15
Hollow Fiber System Studies.....	16
Pharmacokinetics	18
Pharmacodynamics	20
Antibiotic Resistance development.....	20
Pharmacokinetics and Pharmacodynamics Assessment	21
Chapter III. Results	22
Aztreonam-Avibactam Preclinical PK/PD Studies.....	25
PK/PD driver for Aztreonam	28
Avibactam PK/PD index & magnitude.....	33

Sulbactam PK/PD index & magnitude	38
PK/PD driver for Sulbactam	38
ETX2514 PK/PD index & magnitude.....	43
PK/PD driver for ETX2514	44
Chapter IV. Discussion	50
Appendix A. LC-MS/MS conditions	55
Bibliography	57

List of Tables

Table 1: Hollow Fiber Schedule	17
Table 2: MRM transitions.....	20
Table 3: MICs ($\mu\text{g/mL}$) MDR Enterobacteriaceae strains.....	24
Table 4: MICs ($\mu\text{g/mL}$) of <i>A. baumannii</i> strains.	24
Table 5: Goodness-of-fit parameters for clinical strains against Aztreonam-Avibactam..	37
Table 6: Goodness-of-fit parameters for clinical strains against ETX2514Sul.	49

List of Figures

Figure 1: Hollow Fiber Infection Model.....	5
Figure 2: Bacterial growth curve in the Hollow Fiber System.	6
Figure 3: Time vs Concentration compound profile in the Hollow Fiber System.....	7
Figure 4: In-House MIC values for control bacterial strains and compounds	14
Figure 5: Hollow Fiber System Schematics.....	18
Figure 6: Multiple Reaction Monitoring (MRM).	19
Figure 7: Aztreonam concentration-time profile.	26
Figure 8: Avibactam concentration-time profile.....	27
Figure 9: Aztreonam concentration-time profile.	28
Figure 10: Bacterial response to Aztreonam.....	29
Figure 11: Emax model to determine PK/PD relationship for <i>E. coli</i>	31
Figure 12: Emax model to determine PK/PD relationship for <i>K.pneumoniae</i>	32
Figure 13: Emax model to determine PK/PD relationship for <i>E. coli</i> for Aztreonam.....	33
Figure 14: Bacterial response of <i>E. coli</i> to Avibactam.	35
Figure 15: Emax model to determine PK/PD relationship for Avibactam against <i>E.coli</i> . 36	
Figure 16: Sulbactam concentration-time profile.	40
Figure 17: Bacterial response to varying concentrations of Sulbactam against <i>A.baumannii</i> ARC2058.....	41
Figure 18: Emax model to determine PK/PD relationship for Sulbactam against <i>A.baumannii</i>	42

Figure 19: Sulbactam concentration-time profile.	44
Figure 20: <i>A. baumannii</i> ARC5081 response to ETX2514SUL.....	45
Figure 21: <i>A. baumannii</i> ARC5079 response to ETX2514SUL.....	45
Figure 22: Sulbactam and ETX2514 concentration-time profile.....	46
Figure 23: ETX2514 PK/PD E_{max} modeling driver determination for <i>A. baumannii</i> ARC5081.	48

Chapter I.

Introduction

Infectious disease is one of the top ten leading causes of death worldwide (WHO, 2017). Pathogenic microorganisms such as bacteria and viruses can invade the human body which leads to a host immune response. Many of the symptoms that can cause a person to become ill result from the host immune system fighting off the pathogen. These symptoms can vary widely, which can range from a mild cough to a severe condition, such as sepsis or death. The host immune response typically can effectively defend the body against pathogenic microorganisms. However, in some cases the immune system cannot successfully combat the pathogens and medicines, such as antibiotics are needed. Antibiotics can help prevent bacterial infection by either killing bacteria or inhibiting their growth.

The discovery of the first antibiotics, penicillin, has been recognized as the greatest advancement in medicine. Alexander Fleming's discovery of the antibacterial properties of penicillin began the era of antibiotics (ACS, 1999). Cuts and wounds were no longer recognized as life threatening. Modern life saving medical procedures such as surgery became possible with the use of antibiotics. The discovery and success of this miracle drug lead to its overuse. Fleming himself, was one of the first to warn against the potential development of bacterial resistance to penicillin if misused (Aminov, 2010).

Antibiotic resistance existed before the discovery of the first antibiotics. It is the coping mechanism employed by bacteria in order to evade effects of antibiotics. This phenomenon can occur naturally or through random gene mutation due to evolutionary

stress, such as antibiotics. It is the pathogen's defense mechanism. Most antibiotics are naturally derived, such as penicillin. Interactions between pathogens and naturally occurring antibiotics in the environment resulted in pathogens developing an evolutionary mechanism to survive, "survival of the fittest" (Martinez 2012).

Bacteria that produce naturally occurring antibiotics have developed a mechanism in order to protect themselves from the lethal effects of the antibiotics they produce. Resistance mechanisms can vary from modifications of the target, decreasing the affinity of the drug or production of specific enzymes that can modify antibiotics, decreasing their effects. Bacteria utilize two genetic strategies that allow them to coexist with antimicrobial producing organisms. The first is a de novo gene mutation associated with the mechanism of action of antibiotic or its transport into the cell. The second strategy is acquiring foreign resistant genes through horizontal gene transfer from other bacterial species. Horizontal gene transfer occurs when different pathogens interact in the environment and plasmid DNA gets transferred through cell-to-cell interaction (Munita, 2016).

Although there are naturally occurring resistant pathogens, clinically relevant antibiotic resistance often occurs in a hospital setting. These are susceptible strains that become resistant to current antibiotic treatment due to overuse and misuse of antibiotics in the hospital. Pathogens that carry multiple resistant genes are identified as multi-drug resistant (MDR) pathogens, which typically arises from the hospital environment due to increase utilization of antibiotics in this setting. Increase usage and abuse of antibiotics resulted in the rapid development of bacterial resistance due to the greater selective pressure for these strains to survive, resulting in bacterial strains developing resistance to multiple drugs (Struelens, 1998).

The emergence of resistance of pathogenic bacteria against antibiotics has become a worldwide epidemic. Despite this growing problem, the number of new antibiotics in the market continues to decline (Krans, 2014). The World Health Organization (WHO) released their yearly statement urging the nation to become more cautious in antibiotic use and encourages research and development of new classes of antibiotics. Many strains will eventually become resistant to most of the antibiotics currently available in the market. WHO warns that without any new effort, we could face a return to the pre-antibiotic era where a small cut can become life threatening. In 2010, the 10 x '20 Initiative has been put in place in order to combat the alarming decline of antibacterial research (IDSA, 2010). This initiative pushes for a change in global policies to revitalize antibiotic research and development, 10 new antibiotics by 2020.

Major pharmaceutical companies one by one have ventured out of antibacterial research and development. Drugs can take years to develop and can cost companies billions of dollars only to have very few successfully making it to market. Medicines used to treat chronic, life-long diseases are more profitable and a far more attractive market for pharmaceutical companies (Krans, 2014). In order to help progress a successful antibacterial research and development, we need to have a reliable tool that can help predict the success or failure of a candidate compound. In this study, we looked at a dynamic *in vitro* Pharmacokinetics/Pharmacodynamics (PK/PD) infection model that can help predict clinically efficacious dose leading to a successful clinical trial.

PK/PD research models play a crucial role in identifying and developing novel compounds. Pharmacokinetic is the study on what the body does to a drug. Pharmacokinetic study includes understanding the drug's absorption, distribution,

metabolism and excretion of drugs, collectively known as ADME. Pharmacodynamic describes the effect of a drug on the bacterial growth. This provides an insight on the biochemical and physiological effects of the drug and how they affect the growth of bacteria in the body. An understanding of the drug's pharmacokinetic and pharmacodynamic properties allows the basis for the rational therapeutic use of a drug and how to design a new and better therapeutic agent. Pharmacokinetic and pharmacodynamic properties of the drug allow scientists to determine if a candidate compound has the potential to become a lifesaving drug.

Many research laboratories employ both *in vivo* and *in vitro* cell-based assays to help assess a compound's properties. *In vitro* models are time and cost-effective tools in drug discovery. Minimum Inhibitory Concentration (MIC) assay provides a way of quantifying compound potency against a bacterial strain while static or killing kinetics help assess compound efficacy. These models provide useful information in early drug discovery, however, the information from these assays are limited as these assays do not mimic human doses, where drug concentrations fluctuate, but situations where drug concentration remain constant.

The Hollow Fiber System (HFS), dynamic *in vitro* infection models have been developed, capable of mimicking human pharmacokinetics (Blaser, 1985). These models can be utilized to determine the drug exposure needed for efficacy by mimicking fluctuating drug concentration in the system, comparable to how drug concentration fluctuates in the human body.

HFS was initially developed in order to maintain cell culture (Cadwell, 2012). The hollow fiber cartridge is composed of multiple capillary tubes that act as a single dialysis unit. The capillaries consist of hollow fibers, acting as filters. The fibers allow the exchange of fresh media, antibiotics and bacterial metabolites through the extra capillary space while retaining bacteria, resembling a closed system. This ability allowed the development of the hollow fiber system as a PK/PD model. Diffusion of fresh media into the extra capillary space allowed for continuous growth of the cells but also allowed the addition of compounds into the system and the ability to dilute compounds, exposing bacterial culture to fluctuating drug concentration observed in a PK profile (Figure 1).

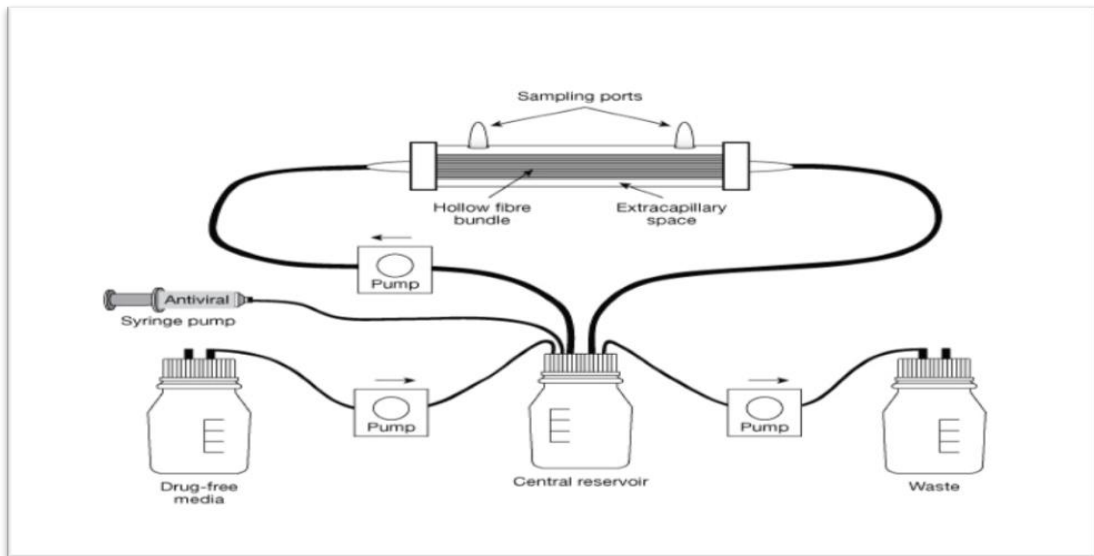


Figure 1: Hollow Fiber Infection Model

McSharry JJ, Deziel MR, Zager K, Weng Q, Drusano GL. Pharmacodynamics of cidofovir for vaccinia virus infection in an in vitro hollow fiber infection model system. Antimicrob Agents Chemother 2009; 53: 129-135

The ability of the system to dilute a fixed reservoir of drug over a specified time allows for simulation of different half-lives. Half-life is the amount of time it takes for the concentration of the drug in the system to reduce in half through elimination. Elimination rate of the drug can be easily controlled in the system by increasing or decreasing the media flow. Samples are collected from the extra capillary space through the sample ports on the hollow fiber cartridges to test for bacterial burden and through the sample port located in the central reservoir for drug concentration (Figure 3). Bacterial burden is assessed by the determining colony forming units (CFU). CFU is a unit of measurement of viable bacterial cells (Figure 2).

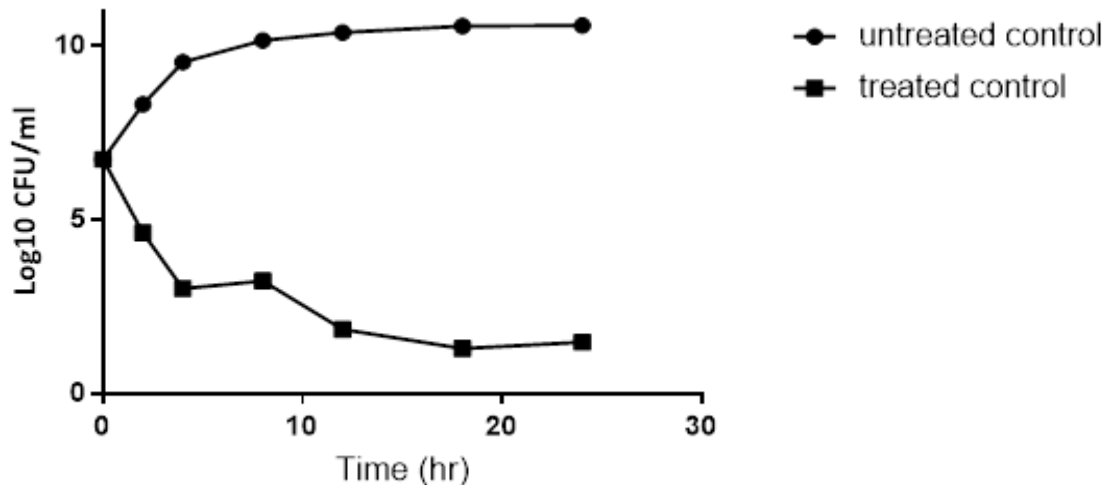


Figure 2: Bacterial growth curve in the Hollow Fiber System.

A schematic representation of an untreated (growth curve) vs treated culture: Bacterial growth profile from HF cartridges comparing bacterial growth with or without the addition of compound. Bacterial burden was assessed by measuring log of the CFU.

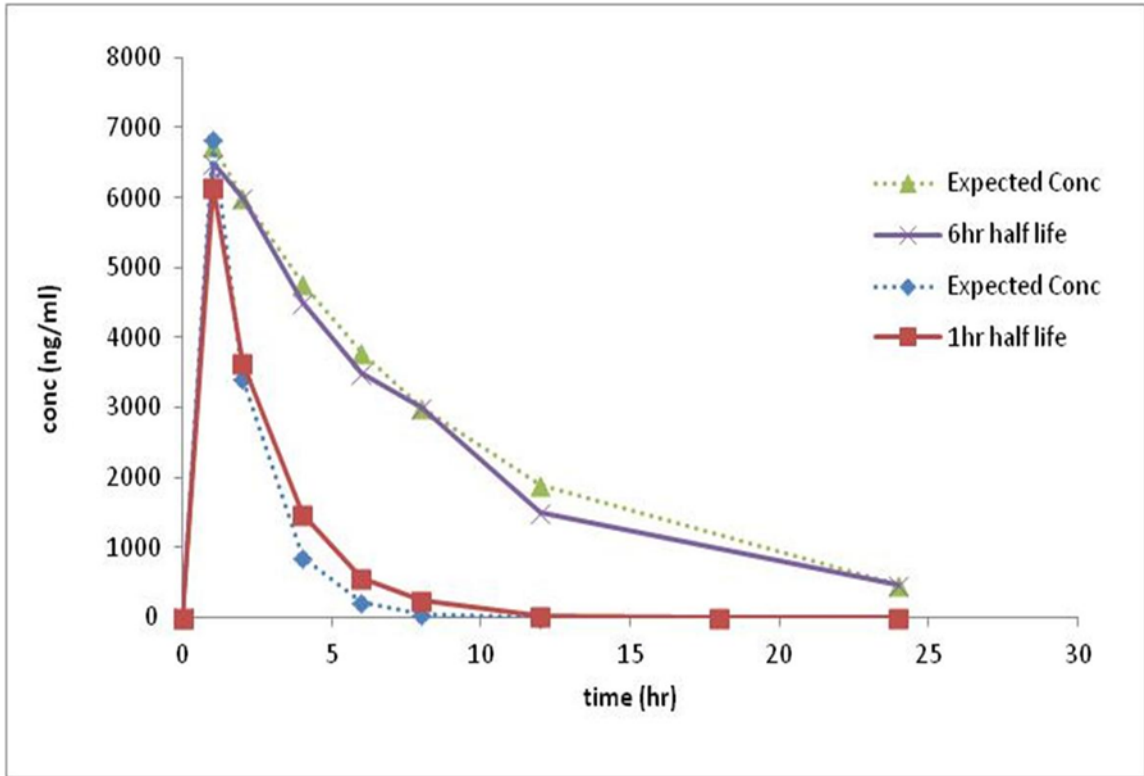


Figure 3: Time vs Concentration compound profile in the Hollow Fiber System.

Levofloxacin, a control antibiotic, profile simulated in the hollow fiber system comparing 1hr and 6hr drug half-life simulation. Elimination rate was controlled through media flow rate.

PK/PD modeling can assist in optimizing drug use by helping design proper dose and regimen. This system can help identify important key PK/PD indices driving the antibacterial properties of a compound (Velkov, 2013). Pharmacokinetic (PK) and Pharmacodynamic (PD) principles help optimize antibiotic treatment by understanding different factors that affect drug response such as onset, magnitude and duration of drug

response (Nielsen, 2013). Utilizing a dose fractionation study can help determine PK/PD indices. Dose fractionation studies are designed by fractionating the dosing intervals throughout the course of a study. A total dose of 24 $\mu\text{g/ml}$ can be given once a day (24 $\mu\text{g/ml}$), twice a day (2 doses of 12 $\mu\text{g/ml}$) or four times a day (4 doses of 6 $\mu\text{g/ml}$). This study design allows for a drug profile with different PK/PD parameters such as identical AUC/MIC over a given time interval but has varying $C_{\text{max}}/\text{MIC}$ across different dosing regimen.

Different PK/PD parameters help determine the driver of efficacy *in vitro*, such as the maximum peak concentration achieved during a single dose ($C_{\text{max}}/\text{MIC}$), the percent time the drug concentration spent above the MIC (%T/MIC) over a 24hr period, or the area under the concentration time curve achieved during dosing relative to MIC (AUC/MIC). These parameters help determine what drives efficacy. It can also help determine the required concentration of drug to achieve an effect or kill.

The hollow fiber System's capabilities can help alleviate some of the burden of running multiple animal studies in drug discovery to determine a drug's PK/PD indices (Drusano, 2004). Previous studies have shown that the hollow fiber system can effectively predict the driver and magnitude of efficacy *in vitro*. It has also been demonstrated as a novel approach in successfully predicting efficacious clinical dose for the combination therapy (Crandon, 2012).

One of the new classes of drugs recently developed is a novel β -lactamase inhibitor, such as Avibactam (Stachyra, 2010). Increase in prevalence of antibiotic resistance in pathogens can be attributed to an enzyme-based mechanism of resistance (Crandon, 2012). β -lactam antibiotics contain a β -lactam ring in their structure, such as penicillin (Kong,

2010). β -lactams have been the go to treatment for bacterial infections since they can treat a wide range of pathogens, however, their overuse resulted in the mutation of β -lactamases. β -lactamases are a family of enzymes responsible for bacterial resistance against a wide variety of β -lactams. The enzyme works by breaking down the β -lactam ring in the structure, rendering the antibiotic inactive. β -lactamases evolved with the continuous use of β -lactams, limiting treatment to very few non- β -lactam antibiotics available (Paterson, 2005). Different classes of β -lactam enzymes have emerged with the extended use of β -lactams. These enzymes fall into different categories such as extended-spectrum β -lactamases (ESBLs), metallo- β -lactamases and AmpC β -lactamases (Oberoi, 2013). Treatment for these β -lactam resistant pathogens are becoming a worldwide concern. Older β -lactamase inhibitors only work against few classes of β -lactamases. β -lactamase producing pathogens are rapidly becoming a clinical concern, prompting further research and development of β -lactam and β -lactamase inhibitor combinations (Singh, 2015).

Development of Avibactam, garnered a significant interest in the scientific community when *in vitro* assays displayed an improvement of β -lactam potency against a wide variety of Gram-negative pathogens when combined with Avibactam, such as Ceftazidime (Livermore, 2011). β -lactamase inhibitors recently developed have a broader spectrum of inhibition compared to older β -lactamase inhibitors. Recent studies have shown that understanding the pharmacokinetics/pharmacodynamics of β -lactam/ β -lactamase combination is crucial in predicting clinically efficacious dose.

Avibactam is first of its class. It is a non- β -lactam β -lactamase inhibitor developed by Actavis and AstraZeneca. This novel β -lactamase inhibitor has been demonstrated to restore activity of β -lactams against bacterial strains that express Class C enzymes (Amp

C-type β -lactamase) and *Klebsiella pneumoniae* carbapenemases (KPC) (Stachyra, 2010). Avibactam became the first β -lactamase inhibitor showing potency against class C-mediated resistance (Lahiri, 2014). The combination, Avibactam-Ceftazidime (AvyCaz) has recently been approved for market to treat Hospital-Acquired Bacterial Pneumonia, Ventilator-Acquired Bacterial Pneumonia, Complicated Urinary Tract infection and Complicated Intra-Abdominal infection.

AvyCaz PK/PD profile was successfully evaluated using the *in vitro* hollow fiber system. Our former Infection group at AstraZeneca was first to test this novel compound combination in the *in vitro* hollow fiber system. This study compared human simulated doses of Ceftazidime and Avibactam both *in vivo* and *in vitro* PK/PD models and showed translatability of data between these models (Crandon, 2012). Data from this study showcased the hollow fiber's ability to help assess pharmacokinetic and pharmacodynamic profile of a compound critical for clinical dosing.

Since the Ceftazidime-Avibactam combination therapy can only cover certain multi-drug resistant strains such as KPCs and Class C enzymes but not New Delhi metallo- β -lactamase (NDM-1). Additional combination therapies were explored. NDM-1 strains are highly resistant to most β -lactams due to their broad range and potent carbapenemase. Aztreonam-Avibactam combination therapy showed great potential (Singh, 2015). This combination therapy showed restoration of efficacy against New Delhi metallo- β -lactamase (NDM-1). This therapy was tested in the *in vitro* hollow fiber system and showed a good correlation of the efficacy observed in the *in vivo* model (Singh, 2015). This combination therapy is currently on Phase 1 clinical trial. These studies showed how the hollow fiber system data were used to optimize clinical doses.

A new class of β -lactamase inhibitor, ETX2514 is currently under development in combination with Sulbactam. ETX2514 is a novel β -lactamase inhibitor that can cover not just class A (SHV, CTX, TEM β -lactamases) and C but also class D (OXA) β -lactamases. Currently marketed β -lactamase inhibitor, such as Avibactam, can only cover class A and C β -lactamases. Class D β -lactamases represent one of the most prevalent mechanisms of resistance in *A. baumannii* associated with multi-drug resistant strains. There is a significant unmet medical need for the treatment of multi-drug resistant *A. baumannii* strain infections. These infections can be attributed to a high mortality rate (CDC, 2017). 60% of these strains are resistant to multiple drug classes, highlighting the need to identify new drugs that can treat these pathogens. Sulbactam is a β -lactamase inhibitor that possesses a weak antibacterial property against pathogens. Preliminary, *in vivo* and *in vitro* data show restoration of Sulbactam antibacterial property when combined with ETX2514 (data not published).

Previous studies have shown the hollow fiber system's potential in helping predict proper clinical doses. The system can be useful in identifying the drug exposure and dosing frequency that will result in an improved therapeutic outcome. Due to the increasing prevalence of multi-drug resistant bacterial strains, many physicians resort to multi drug combination therapy to increase the therapeutic potential of available antibiotics (Nielsen, 2013). This study will demonstrate how the hollow fiber system was a crucial tool in aiding PK/PD modeling in determining proper clinical design for this drug treatment regimen and how combination antibiotic therapies and its impact on dosing regimen and duration has been fully evaluated and how it translates clinically.

Chapter II.

Materials and Methods

The following section details the materials and experimental protocols used for this study. This section outlines the antimicrobial agents and the in-house characterization of bacterial isolates utilized for the Hollow Fiber studies. The system set-up and timeline are also outlined in the section, as well as sample collection and processing and data management and analysis.

Antimicrobials Agents

Commercially available Aztreonam and Sulbactam were purchased from USP (Rockland, MD, USA). Analytical grade Avibactam was provided by Cerexa Inc. (Oakland, CA, USA) while analytical grade ETX2514 was provided by Entasis Therapeutics Inc. (Waltham, MA, USA). Fresh stocks of the drugs were prepared shortly prior to the experiment and reconstituted at X g/L in either Mueller-Hinton broth II (MHBII) (Becton Dickinson, Sparks, MD, USA) or sterile water.

Bacterial isolates

Multi-Drug resistant clinical isolates (Table 3 and Table 4 provided by JMI laboratories (North Liberty, IA, USA) and Entasis Therapeutics (Waltham, MA) culture collection, were tested in the hollow fiber system. Glycerol stocks of the isolates were stored in -80°C. Prior to each experiment, these isolates were sub-cultured twice on Trypticase Soy Agar (TSA) with 5% sheep blood (REMEL, San Diego, CA, USA) and incubated overnight at 37°C.

Characterization of isolates through susceptibility testing

Minimal Inhibitory Concentrations (MIC) of Aztreonam alone, combination Aztreonam/Avibactam, Sulbactam alone and combination Sulbactam/ETX2514 were determined using the Clinical and Laboratory Standards Institute guidelines (CLSI M07-A10) broth microdilution methodology. Varying concentrations of Aztreonam with a fixed 4µg/ml Avibactam and varying concentrations of Sulbactam with a fixed 4µg/ml ETX2514 were tested. The fixed concentration of ETX2514 was previously assessed (data not shown). Compounds were serially diluted 2-fold across each 96-well plate (Corning Inc, Corning, NY) using MHB II. The last column on the 96 well did not contain compound, serving as the growth control for the assay. Compound dilutions were transferred (10µl) into a new 96-well plate after which 90µl of 5×10^5 CFU/ml culture were added. Following incubation between 17.5-18hrs at 37°C, plates were read using a microplate reader (Biotek, Winooski, VT) using an Optical Density (OD) cutoff of 0.065. Any OD greater than 0.065 is considered a growth. Growth is confirmed by eye. MICs were assessed based on the minimum amount of drug needed to inhibit growth of the bacteria. Growth was determined by cloudiness of the growth media or formation of cell layer (“button”) at the bottom of the well. MICs were considered at concentration where no visible growth was observed. An in-house list of bacterial strains and drugs for quality control were used (Figure 4).

MICs (µg/mL) - Exploratory Panel								
	<i>A. baumannii</i>	<i>E. cloacae</i>	<i>E. coli</i>	<i>E. coli</i>	<i>E. coli</i>	<i>E. coli</i>	<i>P. aeruginosa</i>	<i>P. aeruginosa</i>
	OXA-40, OXA-119	Chromosomal AmpC	ATCC 25922	TEM-1	ATCC 25922 toIC	ATCC 25922 toIC +2% Human albumin	PAO1	PAO1 mexABCDXY-
Compound	ARC3495	ARC3528	ARC4	ARC16	ARC4053	ARC4053HA	ARC545	ARC546
Linezolid	>64	>64	>64	>64	8	8	>64	4
Ceftazidime	>64	>64	0.5	0.25	0.25	0.5	1	0.25
	<i>P. aeruginosa</i>	<i>K. pneumoniae</i>	<i>K. pneumoniae</i>	<i>K. pneumoniae</i>	<i>K. pneumoniae</i>	<i>S. aureus</i>	<i>C. albicans</i>	
	hypersensitive strain	SHV-14	ATCC 700603; SHV-18, OXA-2	NVT1001 wildtype	NVT1001 ΔompK35, ΔompK36	USA100 MRSA	ATCC 90028	
Compound	ARC5508	ARC1865	ARC561	ARC6692	ARC6695	ARC3190	ARC1192	
Linezolid	16	>64	>64	>64	>64	2	>64	
Ceftazidime	<.0625	0.25	32	0.125	1	>64	>64	

Figure 4: In-House MIC values for control bacterial strains and compounds

In-House MIC (µg/ml) values for control bacterial strains and compounds used as quality control for MIC assays. ATCC – American Type Culture Collection laboratory strains. Human Albumin is added to test for any binding affinity of the compound. MRSA – Multi-resistant S. aureus

Dose Response and Dose Fractionation Study Design

A series of dose response and dose fractionation experiments were conducted with various strains of bacteria, in order to assess the PK/PD indices, drug vs pathogen, relationship for the target. Dose response studies involved dosing the system once a day with varying drug concentrations to determine at what drug concentrations we observe no-kill (bacterial growth) and varying bacterial response. Dose fractionation studies involve dosing the system multiple times a day with the same total dose chosen based on the Dose response data while varying the dose intervals throughout the course of the study. The ideal study design involves drug concentrations with varying regimens and varying bacterial response. Systems were dosed using a programmable (Harvard Apparatus, Holliston, MA) syringe pump to achieve a C_{max} at 1hr and mimicking 1hr infusion duration. The rate of

drug-free media diluting the media containing drug in the system allows for the system to mimic different drug half-lives, simulating a single-compartment model with exponential elimination.

A half-life of 2hrs was selected to mimic actual human half-lives of Aztreonam and Sulbactam (Drugs@FDA, 2018). The system was serially sampled to determine simulated drug exposure and bacterial burden over 24hr in all experiments. The PK/PD parameters that correlated with *in vitro* efficacy were determined. Doses were administered once daily (q24h), every 12 hours (q12h), or every 6 hours (q6h) to vary the AUC/MIC, C_{\max} /MIC, and %T>MIC across the cartridges. These are the different PK/PD parameters used in this study to help determine the driver of efficacy *in vitro*. C_{\max} /MIC is the maximum drug peak concentration achieved during a single drug dose. Percent time above the MIC (%T>MIC) is the time the drug concentration spent above the MIC over a 24hr period, or the area under the concentration time curve achieved during dosing relative to MIC (AUC/MIC).

Hollow Fiber system set-up

All studies were conducted in a Biosafety level 2 laboratory. The hollow fiber system components and media were sterilized using an autoclave. System set-up was conducted under a biosafety cabinet to ensure that the system remained sterile.

The system was set-up with the fresh media bottle containing sterile MHBII and waste bottle placed on customized shelving. A peristaltic pump (Cole Palmer, Vernon Hills IL USA) allowed continuous flow of drug-free media replacing any drug containing media in the system. Customized masterflex platinum cured silicon tubing (Cole Palmer, Vernon Hills IL USA) connecting the media and waste bottle to each cartridge were looped through

a reach-in incubator. Cartridges were set in a duet pump (Fibercell Systems, Frederick, MD). System was set-up with the incubator set at 37°C for 48hrs prior to the beginning of the study, to provide enough time for the hollow fiber cartridges to equilibrate with MHBII and assess the aseptic condition of the system. Studies were run for 24hrs in a 37°C humidified environment.

Drug system compatibility was first tested to determine the optimum cartridge type for each specific drug. Two different types of hollow fiber cartridges, cellulosic and polysulfone were tested to determine drug compatibility with the system. These cartridges are identical except for the material used to make the hollow fibers. Pretest involves running the drug in the system alone without any culture. Compatibility determines whether the drug show non-specific binding in the system. This ensures that minimal drug is lost in the hollow fiber system.

Data from the pretest study showed that Cellulosic was the optimal cartridge type compatible with all drugs tested here (data not shown). Drug concentration recovery was $\geq 80\%$ of the target concentration.

Hollow Fiber System Studies

At 24hr before the start of the study, frozen glycerol stocks of bacterial culture were passaged unto a fresh TSA plate and incubated at 37°C for at least 18 hrs. On the day of the experiment, 20ml of MHBII was inoculated with the overnight bacterial culture from the plate and incubated shaking for 1hr at 37°C, to allow bacteria to grow to log phase, OD 0.06-0.09. A turbidity meter (Beckman Coulter, Brea, CA, USA) was used to determine culture OD, a range of 0.06 – 0.09. The culture was diluted with fresh MHBII

to achieve target colony forming unit (CFU), 1×10^6 CFU/ml. A volume of 15ml of bacterial suspension was inoculated into the extra capillary space of the hollow fiber system. The culture was incubated in the cartridge for 1hr in order for the culture to equilibrate with the system. Subsequently, a bacterial sample was collected and plated on TSA plates with 5% sheep blood. This served as the starting density for the study, which is critical when assessing PK/PD data. After sampling, drug was infused to achieve the desired PK profile and regimen for each hollow fiber cartridge. The doses were administered via syringe pump.

Table 1: Hollow Fiber Schedule

Time (h)	dosing drug (pump)		Sample Compound	Sample Bacteria
			All	All
prep	Wednesday	6:30 AM		
inoc		7:00 AM		
-1		8:00 AM		
0		9:00 AM	Dose X	X
1		10:00 AM	Peak X	
2		11:00 AM	X	X
3		12:00 PM		
4		1:00 PM	X	X
5		2:00 PM		
6		3:00 PM	Dose X	X
7		4:00 PM	Peak X	
8		5:00 PM		X
9		6:00 PM		
10		7:00 PM		
11		8:00 PM		
12		9:00 PM	Dose X	X
13		10:00 PM	Peak X	
14		11:00 PM		
15	Thursday	12:00 AM		
16		1:00 AM		
17		2:00 AM		
18		3:00 AM	Dose X	X
19		4:00 AM	Peak X	
20		5:00 AM		
21		6:00 AM		
22		7:00 AM		
23		8:00 AM		
24		9:00 AM	X	X

HFS sample dosing schedule. Sampling is based on the frequency of dosing.

The system was serially sampled to determine both bacterial density and compound concentration (Table 1).

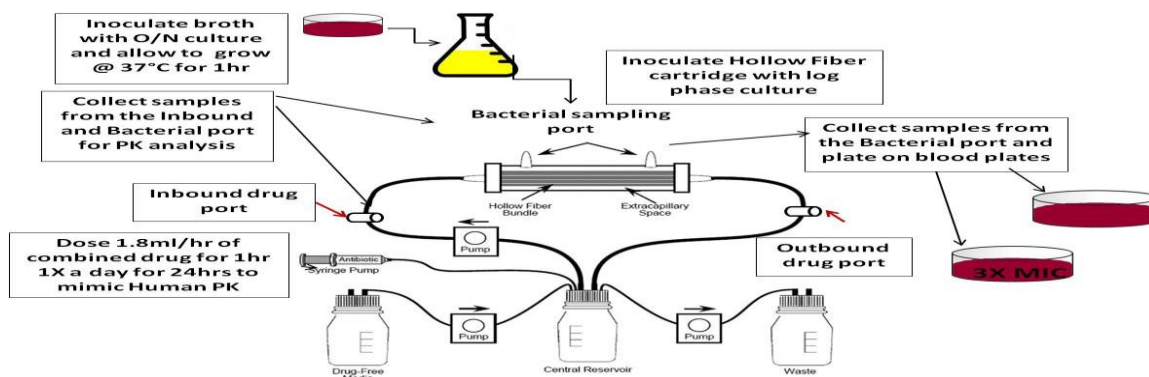


Figure 5: Hollow Fiber System Schematics

Pharmacokinetics

Samples from the reservoir bottle (PK samples) (200 μ l) were collected over a 24hr time period to determine drug exposure in all experiments. A standard curve with a range of 1-10,000 ng/ml for each compound being analyzed, was used to determine drug concentration in the system. Samples were further diluted to ensure sample concentration were in the dynamic range of the assay before being directly injected onto the LC-MS/MS instrument. Calibration standards were prepared (1, 2.5, 5, 10, 25, 100, 500, 1000, 5000 and 10000 ng/ml) by serial dilution in 1:1 MHBII broth:mouse plasma (BioIVT, Westbury, NY). Compound concentrations were determined by liquid chromatography-mass spectrometry (LC-MS/MS) (Sciex API 5000 and Sciex API 6500) to confirm the concentration-time profile (Table 2)(Appendix A).

A volume of 50 μ l was transferred into 96 deep-well round-bottom plates (Corning Inc, Corning, NY). The samples were precipitated using 150 μ l acetonitrile containing 250ng/mL internal standard, Carbutamide (Sigma Aldrich, St. Louis, MO). Plates were mixed using a multi-tube vortexer (VWR International, Radnor, PA) for 20 seconds with

motor speed set at 4 at room temperature and centrifuged at 4000 x g for 10 minutes using Centrifuge 5810R (Eppendorf, Hamburg, Germany). Supernatant (120 µl) was transferred to a clean 1ml 96-deep well round-bottom DNase/RNase free collection plate (Thermo Scientific, Rochester, NY) Samples were analyzed by injection of 5.0 µl onto LC-MS/MS.

Sciex API 5000/ Sciex API 6500, controlled by Analyst v1.6.1, was used for the data acquisition and the quantification of compound concentration. Atlantis T3, 3µ, 50 x 3.0mm column was used to analyze all the samples, using a column temperature of 35°C with a flow rate of 1.2ml/min. Water + 0.1% formic acid was used for mobile phase A and Acetonitrile + 0.1% formic acid for mobile phase B. Chromatographic separation of analytes was achieved using a gradient of mobile phase A and B consisting of solvents to help elute samples into the column and optimized to achieve good chromatographic peaks. (Figure 6, Table 2).

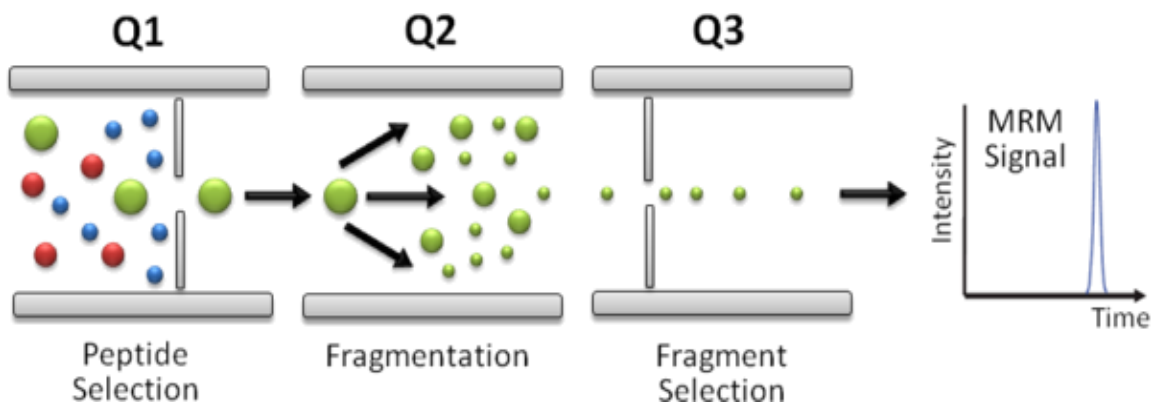


Figure 6: Multiple Reaction Monitoring (MRM).

Multiple Reaction Monitoring (MRM) use the signal of selected compound fragment ions for quantification. Q1 selects a parent peptide ion, Q2 fragments the peptide, and Q3 selects a specific fragment ion for the detector. Q1 is based on the compounds molecular weight. <http://www.inf.fu-berlin.de/lehre/WS14/ProteomicsWS14/LUS/lu6a/345/index.html>

Table 2: MRM transitions.

Drug ID	Q1	Q3	DP	CE	CXP
Aztreonam	433.94	95.80	-30	-20	-13
Avibactam	264.10	96	-60	-20	-15
ETX02514-009	276.10	96.1	-40	-27	-15
ETX-010151 (Sulbactam)	232.10	140.0	-40	-25	-15
Carbutamide (IS)	270.00	171.00	-55	-25	-10

MRM transitions used for each compound ran in the LC-MS/MS instrument.

Pharmacodynamics

The bacterial burden (CFU/mL) (PD results) was measured by sampling (500 μ l) from the extra-capillary space of the hollow-fiber cartridge at various time points. Bacterial samples were then diluted (serial 10-fold dilutions) into MHBII, 100 μ l of bacterial samples were diluted into 900 μ l MHBII of which 100 μ l volumes were plated on TSA plate. The plates were then incubated for 24hr at 37°C after which visible colony-forming units were counted. CFU is plotted on a logarithmic scale and reported as log₁₀ CFU, to easily assess when a high number of bacteria is reported (Figure 10). The delta CFU population was calculated as the change in total microbial population between time 0 hr (starting inoculum) and 24 hr.

Antibiotic Resistance development

To determine development of bacterial resistance in the system, 24hr samples were plated on drug-supplemented agar plates made from Mueller Hinton Agar (MHA) (Becton Dickinson, Sparks, MD, USA). Melt MHA in the microwave. Set molten agar in a 55°C water and wait until the temperature equilibrate. Add compound concentration 4X the MIC of the β -lactam and a 4 μ g/ml of the β -lactamase inhibitor. MIC is based on the combination MIC of the β -lactam and β -lactamase inhibitor. (Table 3 and Table 4). Allow enough time

for agar to solidify and the agar surface to dry before plating bacterial samples. Serial 10-fold dilutions of the 24hr bacterial samples were prepared by dilution of 100 µl of bacterial sample into 900 µl of which 100 µl was plated on drug-supplemented agar plates, which were subsequently incubated at 37°C for 72 hr. Several colonies formed on the drug plates (at least 3 colonies) were passaged on drug-free TSA plates twice, followed by transfer onto drug plates to confirm stability of drug resistance. Any resulting colonies on the drug plates were tested for a shift in MIC using the broth microdilution method following guidelines of document CLSI M07-A10. (CLSI 2006)

Pharmacokinetics and Pharmacodynamics Assessment

PK/PD modeling and simulations were conducted by fitting the PK results to a one compartment model with an infusion input Phoenix version 6.2.0 (PK Model 2- IV-infusion) WinNonlin software (Pharsight, Mountain View, CA). The PD results were measured by taking the total bacterial population difference between the 0hr (starting burden) with the 24hr bacterial burden (delta population). The observed drug concentration-time profiles over 24 hr and delta CFU population were used to calculate the AUC/MIC, C_{max}/MIC , and %T>MIC. The concentration drug profile was calculated as described in the equation below,

$$C(t) = (((D/TI)/V)/K_{10}) * e^{(-K_{10} * T_{STAR})} - e^{(-K_{10} * t)}$$

where the drug concentration in the compartment, $C(t)$, is calculated based on the drug infusion duration, (D), time of drug infusion (TI), total system volume (V) and K_{10} (elimination rate constant). The initial parameter estimates for V and K_{10} were 223 mL and 0.385, respectively.

Sigmoidal E_{\max} model (Model 108) WinNonlin was used to calculate the PK/PD index that was most closely associated with efficacy and its magnitude. The data was modeled using a sigmoid E_{\max} model described by the following equation,

$$E = E_{\max} - (E_{\max} - E_0) * (C^N / C^N + EC_{50}^N)$$

where E_{\max} is the maximum bacterial growth observed in the absence of drug; E_0 is the maximum kill, EC_{50} is the concentration that gives 50% of response, and N is the Hill factor. PK/PD endpoints of bacterial stasis and 1-log kill were determined from the fitted data. Bacterial stasis is defined as no-change in bacterial burden from the onset and end of a study.

The goodness of fit was determined by evaluating the variability in the model calculated parameters and an analysis of the weighted residuals (R^2 and WSSR). The coefficient of determination (R^2), is the proportion of the variance based in the dependent variable based on the predicted variable. The closer R^2 to 1.0 the better the coefficient (Nielsen, 2011). Weighted Sum of Squared Residuals (WSSR) is the measured deviation of the observed value based on the predicted value utilizing the selected model. A smaller number represents better correlation of the predicted and observed data (Yan, 2012).

Chapter III.

Results

Bacterial strains utilized for these studies were chosen based on their MIC and their β -lactamase content. A range of strains were chosen based on the compound's MIC90.

MIC₉₀ is the minimum concentration of compound that can cover 90% of the culture panel tested. Strains in the culture panel are chosen based on their MIC profile against different comparator drugs. The MIC values of the bacterial strains used in the PK/PD studies are shown in Table 3 and Table 4. The *K. pneumoniae* and *E. coli* strains evaluated in this study had an MIC value between 16 to 256 µg/ml against Aztreonam and an MIC of greater than 8 µg/ml for Avibactam alone. Addition of Avibactam helped improved the Aztreonam activity against these clinical strains. The combination of Aztreonam and 4 µg/ml Avibactam decreased the *K. pneumoniae* MIC by at least 512-fold while the *E. coli* MIC decreased by at least 32 fold. MIC data were generated in-house.

The Sulbactam MIC for *A. baumannii* strains evaluated for this study ranged from 2 – 32 µg/ml, while the ETX2514 MIC value was greater than 32 µg/ml. The combination of Sulbactam with 4 µg/ml ETX2514 decreased the MIC by at least 8 fold to- 64 fold for the highly resistant strains such as ARC3486 and ARC5079.

The 4 µg/ml concentration for the β-lactamase inhibitor, Avibactam and ETX2514, was selected based on a predictor panel of bacterial strains previously described for other BL/BLI combinations against β-lactamase-producing Gram-negative bacteria. The predictor panel consists of clinical isolates that included a variety of bacterial strains that are intrinsically susceptible, intrinsically resistant and have various susceptibilities based on the different types and amount of β-lactamase the strain produces (Bradford, 1993). DNA sequencing confirmed the β-lactamase present in each strain evaluated and a β-lactamase assay was utilized to confirm expression of the β-lactamase (Data not shown).

Table 3: MICs ($\mu\text{g/mL}$) MDR Enterobacteriaceae strains.

Pathogen	Strain #	β -lactamase content	Type	Aztreonam	Avibactam	Aztreonam + Avibactam (4 $\mu\text{g/ml}$)
<i>E. coli</i>	ARC4		Susceptible	0.25	>8	-
<i>K. pneumoniae</i>	ARC3803	NDM-1, CTX-M-15, OXA-1, SHV-1, TEM-1	MDR	256	>8	0.25
<i>K. pneumoniae</i>	ARC3602	NDM-1, CTX-M-15, SHV-11, TEM-1, CMY-6	MDR	256	>8	0.5
<i>K. pneumoniae</i>	ARC3802	NDM-1, CTX-M-15, SHV-11, SHV-2a, TEM-1	MDR	128	>8	0.125
<i>E. coli</i>	ARC3805	NDM-1, TEM-208, OXA-1, OXA-2, CTX-M-15, CMY-4	MDR	>256	>8	4
<i>E. coli</i>	ARC3807	NDM-1, TEM-1, SHV-12, OXA-9, CMY-42	MDR	>256	>8	8
<i>E. coli</i>	ARC3600	NDM-1, OXA-1, CMY-6	MDR	16	>8	0.125

MICs ($\mu\text{g/mL}$) MDR Enterobacteriaceae strains utilized in PK/PD studies. Multi-Drug Resistance (MDR).

Table 4: MICs ($\mu\text{g/mL}$) of *A. baumannii* strains.

Strain	β -lactamase content	Type	ETX2514	Sulbactam	Sulbactam + ETX2514 (4 $\mu\text{g/ml}$)
ARC2058	OXA-95	Susceptible	>32	2	1
ARC3484	OXA-23, OXA-64, TEM-1	MDR	>32	16	0.5
ARC3486	OXA-66, OXA-72, TEM-1	MDR	>32	32	0.5
ARC5079	OXA-65, OXA-72	MDR	>32	32	1
ARC5081	OXA-23, OXA-66	MDR	>32	8	2
ARC5091	OXA-23, OXA-78	MDR	>32	8	1

MICs ($\mu\text{g/mL}$) of *A. baumannii* strains utilized in PK/PD studies.

Aztreonam-Avibactam Preclinical PK/PD Studies

One of the aims of this study is to determine whether the PK/PD index and magnitude of Aztreonam against metallo- β -lactamase (MBLs) and Extended spectrum β -lactamases (ESBLs) producing pathogens such as *E. coli* and *K. pneumoniae* will change when co-administered with Avibactam. The %T>MIC is a well-established PK/PD index for β -lactam antibiotics. Against susceptible strains, Aztreonam has demonstrated, ~50% Time above MIC (%T>MIC) as the PK/PD magnitude required for efficacy (Vinks, 2007).

The hollow fiber system was dosed with different concentrations of Aztreonam, administered every 24hr, every 12hr, every 6hr and mimic a 2hr half-life in the system. The hollow fiber system and LC-MS/MS have a +/- 20% error and the difference between the observed and the simulated Aztreonam data was less than 25% between the profile half-lives in the hollow fiber system for each cartridge ran in the study (Figure 7). The Avibactam concentration was kept constant in the system through constant infusion (Figure 8).

Figure 7A

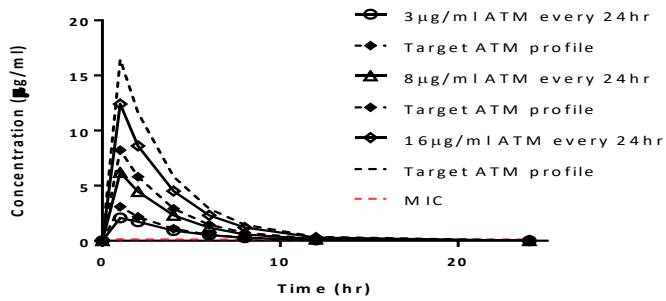


Figure 7B

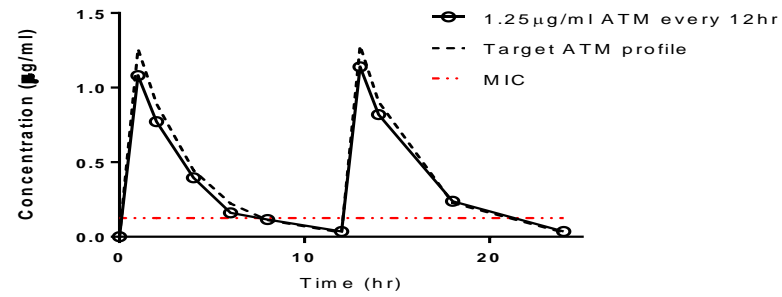


Figure 7C

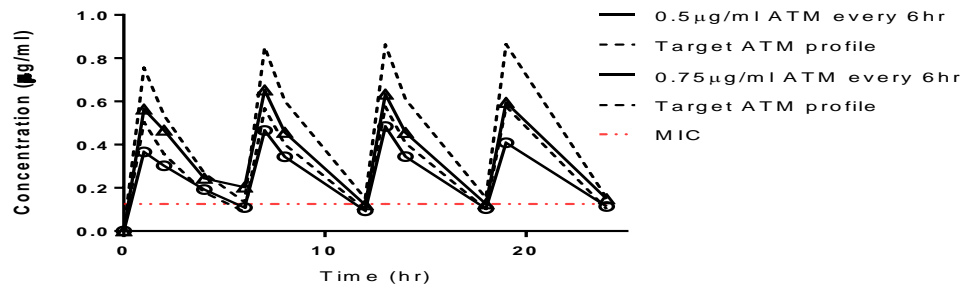


Figure 7: Aztreonam concentration-time profile.

*Aztreonam concentration-time profiles in the hollow fiber System. Solid line represent Aztreonam profile observed in the hollow fiber System. Fluctuating dash line represents target Aztreonam profile. Graphs are labeled based on the targeted C_{max} and regimen. Profiles represent concentrations in different cartridges infected with different strains of *K. pneumoniae* and *E. coli*. Continuous dash lines represent the MIC value.*

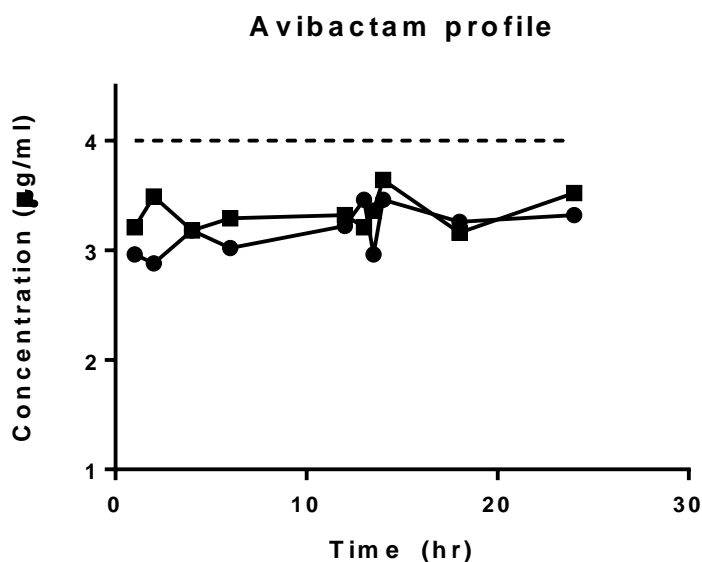


Figure 8: Avibactam concentration-time profile.

Avibactam concentration-time profiles in the Hollow Fiber System. System was dosed as a continuous infusion targeting 4 µg/ml at steady state. Solid line represent Avibactam profile observed in the hollow fiber system from two different cartridges to show reproducibility of the drug profile in the system. Dash line represent target Avibactam profile.

Samples were collected in the reservoir bottle and the bacterial compartment of the system to demonstrate uniformity of the compound concentration in the system (Figure 5). When Aztreonam was dosed alone in the system, Aztreonam was hydrolyzed in the bacterial compartment containing *K. pneumoniae* ARC3802 (Figure 9). However, when Aztreonam and Avibactam were dosed in combination, the Aztreonam concentrations measured in the bacterial compartment of the system was consistent with the compound concentration observed in the central reservoir (Figure 5). Degradation of Aztreonam was not observed in the bacterial compartment when dosed in combination with Avibactam which demonstrates Avibactam's ability of protecting Aztreonam against enzyme β -

lactamase hydrolysis (Figure 9). The Avibactam dose level tested in the system was sufficient in protecting Aztreonam based on PK profile showing minimal Aztreonam degradation. Similar effects were observed for other strains tested in the system (Data not shown) as well as other BL/BLI combination tested in the hollow fiber system (Crandon, 2012).

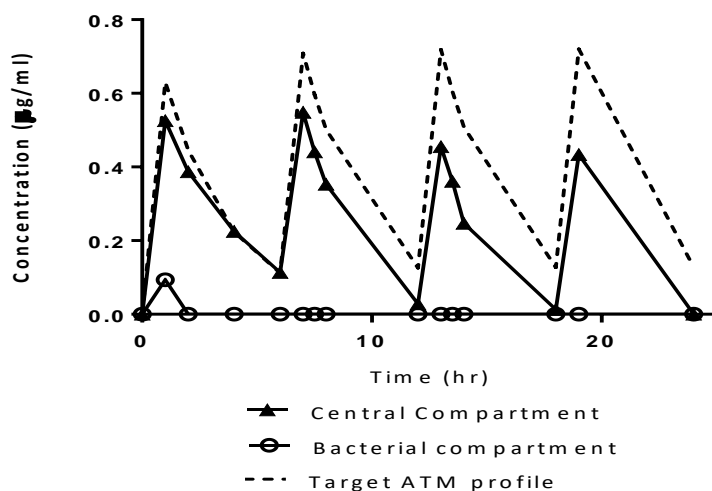


Figure 9: Aztreonam concentration-time profile.

Aztreonam concentration profile in the Hollow Fiber System in the absence of Avibactam. In the absence of Avibactam, degradation of Aztreonam was observed in the bacterial compartment of the hollow fiber system. System contained K. pneumoniae ARC3802.

PK/PD driver for Aztreonam

Aztreonam and Avibactam was efficacious against *K. pneumoniae* and *E. coli* Multi-Drug Resistant clinical strains in the hollow fiber system. Rapid kill of at least 3 log₁₀ for both isolates the first 4hr of the study was observed with varying Aztreonam

concentration (0.75 - 18 $\mu\text{g/ml}$ dosed every 6, 12 and 24hr) combined with 4 $\mu\text{g/ml}$ constant infusion of Avibactam. Bacterial response of *K. pneumoniae* ARC3802 is shown on Figure 10 (Singh, 2015). Same response was observed for *K. pneumoniae* strains ARC3803, and ARC3602 and *E. coli* strains ARC3805, ARC3807 and ARC3600 tested in the system (data not shown). Aztreonam dosed alone at the target dose concentration of 0.75 $\mu\text{g/ml}$ every 24hr, designed to give an exposure of 50% T>MIC, show minimal effect in the bacterial growth curve (Figure 10). This result was consistent with these strains having a high MIC against Aztreonam (Table 3). The same was observed for the Avibactam alone growth curve (Figure 10).

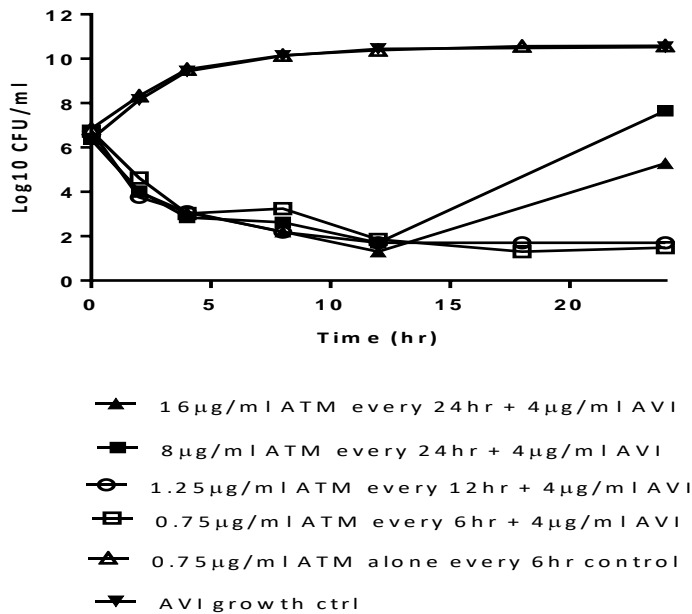
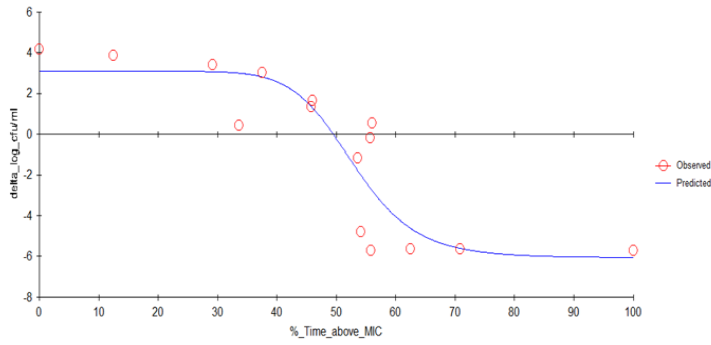


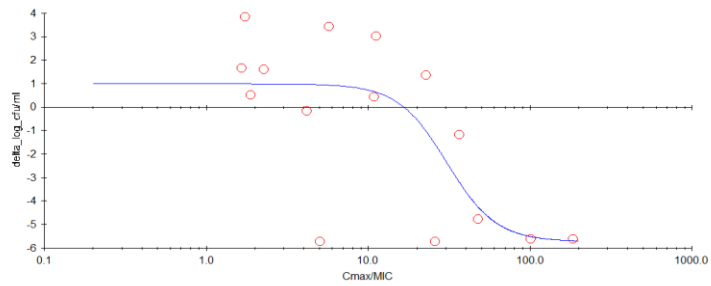
Figure 10: Bacterial response to Aztreonam.

*Bacterial response to varying concentrations of Aztreonam (ATM) in the presence of 4 $\mu\text{g/ml}$ constant infusion of Avibactam (AVI) against MDR isolate *K. pneumoniae* ARC3802. Graphs are labeled based on the targeted C_{max} and regimen.*

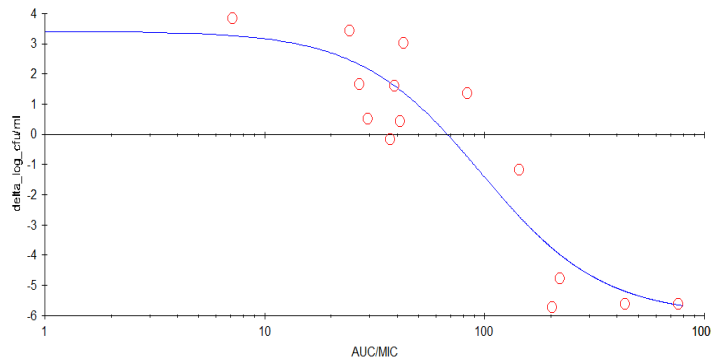
Bacterial response data show that once a day dosing of Aztreonam (16 μ g/ml ATM every 24hrs) was not sufficient to suppress bacterial growth for 24hr. As the drug concentration dipped below the MIC value, the bacterial population start to regrow (Figure 7A). However, dosing Aztreonam more frequently even at a lower concentration (0.75 μ g/ml ATM every 6hrs) show a better suppression of bacterial growth in 24hr (Figure 10). This study show that Aztreonam needs to maintain a dose concentration above the MIC at a certain % Time of the study (24hr) to see efficacy. The PK/PD index for Aztreonam in combination with Avibactam demonstrates %T>MIC. Data of Aztreonam against a susceptible strain (*E. coli* ARC4) suggest that PK/PD index for Aztreonam does not change in the presence of Avibactam (Figure 11). The hollow fiber study show that the PK/PD index for *K.pneumoniae* ARC3802 is 50% T>MIC (Figure 12) while *E.coli* ARC 3600 show a slightly higher %T>MIC at 55% (Figure 13).



E. coli ARC4
 $R^2 = 0.88$



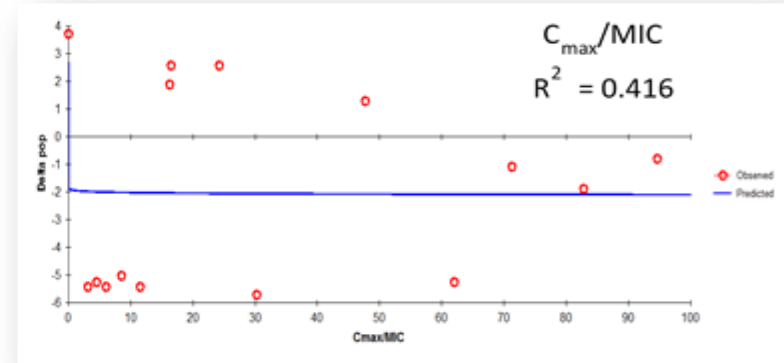
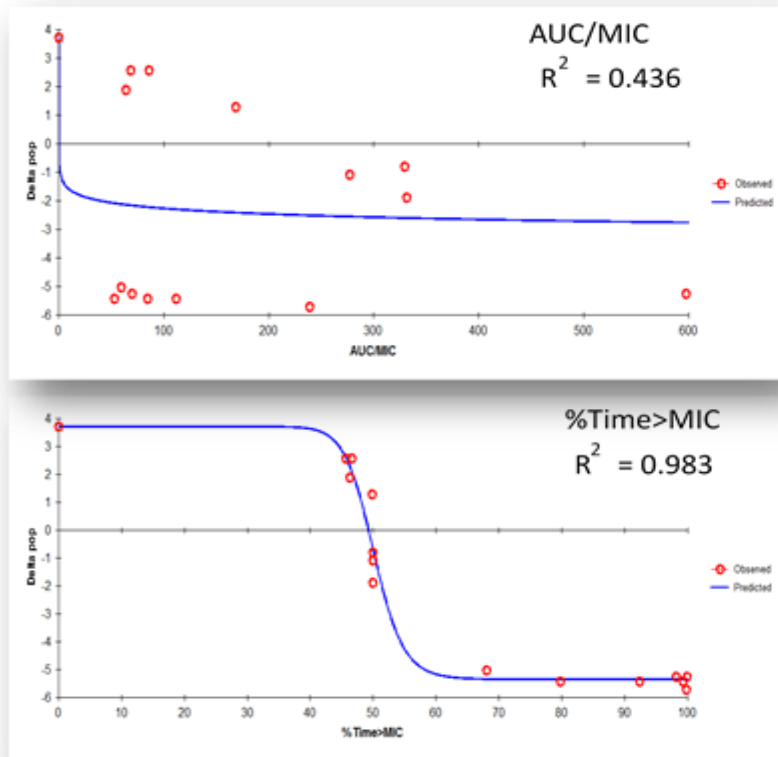
E. coli ARC4
 $R^2 = 0.69$



E. coli ARC4
 $R^2 = 0.82$

Figure 11: Emax model to determine PK/PD relationship for *E. coli*.

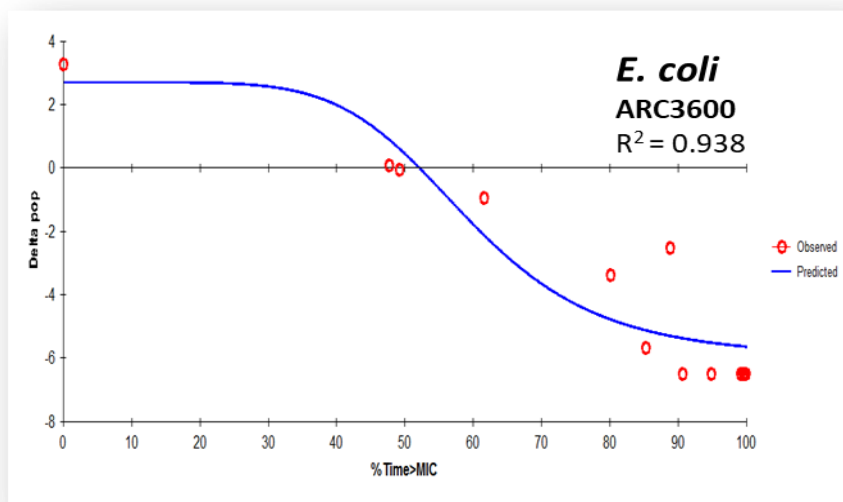
Emax model to determine PK/PD relationship comparing AUC/MIC, C_{max}/MIC and $\%T > MIC$ for Aztreonam against a susceptible strain, *E. coli* ARC4 in the hollow fiber system. Circles represent the observed data while the continuous line represent the predicted best-fit model.



%Time > MIC			
Parameter	Estimate	Std error	CV%
Stasis	49.29	0.36	0.72
1 Logdrop	50.34	0.44	0.88
2 Logdrop	51.41	0.69	1.35

Figure 12: Emax model to determine PK/PD relationship for *K.pneumoniae*.

*Emax model to determine PK/PD relationship comparing AUC/MIC, C_{max}/MIC and %T>MIC for Aztreonam in the presence of 4 μ g/ml constant infusion of Avibactam against *K.pneumoniae* ARC3802 in the hollow fiber System. Circles represent the observed data while the continuous line represent the predicted best-fit model. (Singh, 2015).*



%Time > MIC			
24-h Endpoint	Estimate	Std error	CV%
Stasis	45.31	4.31	9.50
1 Logdrop	55.08	5.51	10.00
2 Logdrop	55.99	3.77	6.73

Figure 13: Emax model to determine PK/PD relationship for *E. coli* for Aztreonam.

Emax model to determine %T>MIC for Aztreonam in the presence of 4µg/ml constant infusion of Avibactam against E. coli ARC3600 in the hollow fiber System. Circles represent the observed data while the continuous line represent the predicted best-fit model. (Singh, 2015).

Avibactam PK/PD index & magnitude

To determine the PK/PD index and magnitude for Avibactam, a fixed dose of Aztreonam, which covers 50 %T>MIC of the combination MIC, was tested in the hollow fiber system in combination with varying dose regimen of Avibactam. Aztreonam PK/PD data showed 50 %T>MIC, combined with a 4µg/ml constant dose of Avibactam was

adequate for efficacy (Figure 14).

Determining PK/PD driver and index relies on an MIC value of a drug. However, since Avibactam does not have any intrinsic antibacterial property against the strains tested in the hollow fiber system (Table 3), a slightly different PK/PD index was utilized (Figure 15), Time above Critical Threshold ($T > C_T$) was applied to determine the avibactam PK/PD driver. Frequent dosing of avibactam in the presence of Aztreonam showed a time-dependency of the PD effect which links the $T > C_T$ to efficacy (Figure 15). $T > C_T$ suggests that in order to achieve efficacy in the system, we need to keep Avibactam concentration at a certain level throughout the study (24hr). A range of (0.5 to 4 $\mu\text{g/ml}$) critical concentrations was investigated in the hollow fiber system. These are the threshold values utilized to determine the PK/PD index. To determine the goodness of fit parameters (R^2 and WSSR), the $\Delta \log_{10}\text{cfu/mL}$ at 24 hr and $\% T > C_T$ were utilized (Singh, 2015). Additional exposure parameters such as C_{max} , AUC were analyzed but found no correlation (Figure 15).

A single high dose of Avibactam (12 $\mu\text{g/ml}$ and 16 $\mu\text{g/ml}$ q24h) was not sufficient to suppress growth in the hollow fiber system. By 12hrs rapid bacterial growth was observed (Figure 14). Frequent dosing also showed no improvement in efficacy with a low avibactam dose (2-4 $\mu\text{g/ml}$ q6h). This suggests that a once a day high dose of avibactam was not sufficient in inhibiting β -lactamase production in these strains (Singh, 2015). More frequent dosing at an optimal dose between 6-8 $\mu\text{g/ml}$ (q12h) and 8 $\mu\text{g/ml}$ (q6h) Avibactam showed suppression of bacterial growth over 24hr.

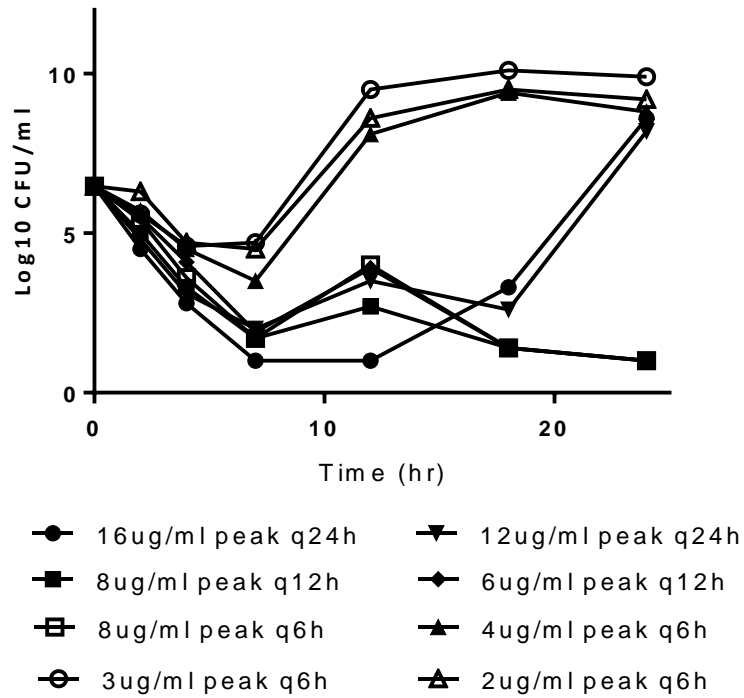
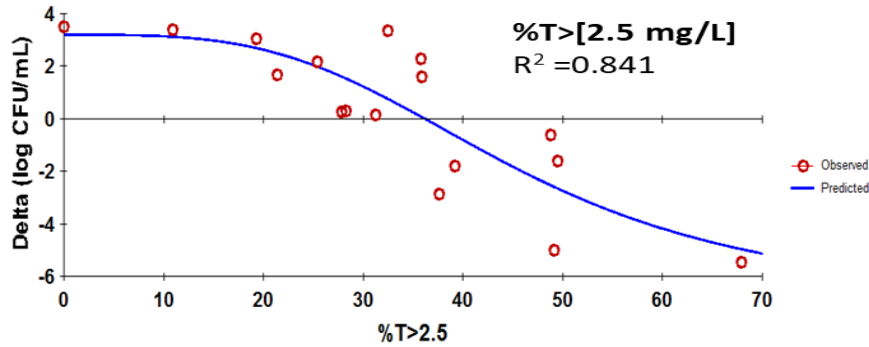
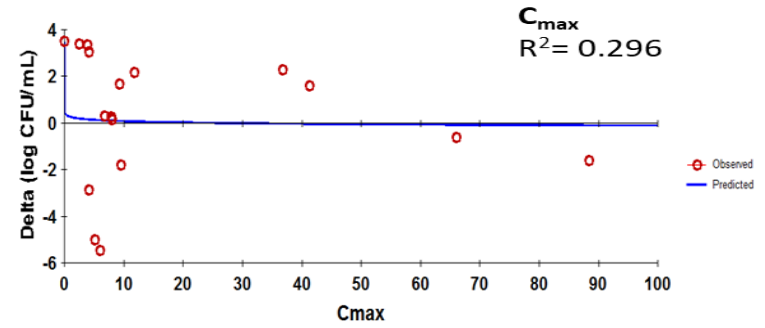
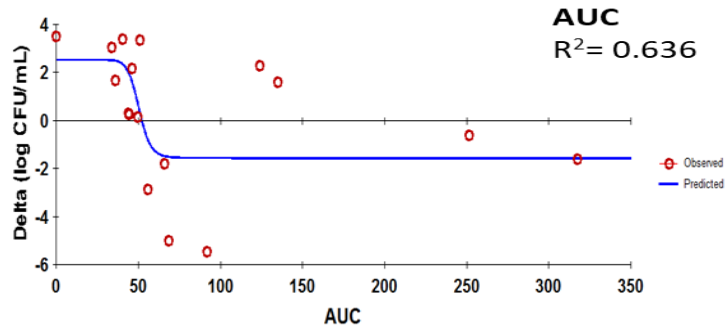


Figure 14: Bacterial response of *E. coli* to Avibactam.

Bacterial response to varying concentrations of Avibactam in the presence of 50% T>MIC of Aztreonam against E. coli ARC3600. Graphs are labeled based on the targeted C_{max} and regimen.

Strains tested in the hollow fiber system showed a maximum correlation of efficacy with a critical threshold of 2.5µg/ml. Lower and higher critical threshold concentrations show lower R² value which suggests lower correlation with efficacy (Table 5). *E. coli* strains show maximum efficacy at a C_T of 2.5 µg/ml while some *K. pneumoniae* showed high correlation between 2.5 and 3 µg/ml. R² for both threshold was comparable, so the same dose would suffice for both. *In vivo* data correlates with observed data from the hollow fiber system (Data not shown). With this correlation, the projected clinical dose for avibactam was targeted at 2.5 µg/ml C_T (Singh, 2015).



%Time > [2.5mg/L]	Estimate	Std Dev	CV%
24-h Endpoint			
Stasis	36.10	2.81	7.77
1 Logdrop	40.92	3.28	8.01
2 Logdrop	45.91	4.18	9.10

Figure 15: Emax model to determine PK/PD relationship for Avibactam against *E.coli*.

Emax model for AUC/MIC, C_{max}/MIC and %T>MIC for Avibactam in the presence of fixed dose of Aztreonam against E.coli ARC3600 in the hollow fiber System. Circles represent the observed data while the continuous line represent the predicted best fit-model (Singh 2015). Unit used for modeling was mg/L which is equivalent to µg/ml.

Table 5: Goodness-of-fit parameters for clinical strains against Aztreonam-Avibactam.

Clinical isolates	Parameters	Critical threshold (C _T) values			
		1 mg/L	2 mg/L	2.5 mg/L	3/4 mg/L
<i>K. pneumoniae</i> ARC3802	R ²	0.82	0.83	0.76	NA
	WSSR ^a	69	67	91	NA
<i>K. pneumoniae</i> ARC3602	R ²	0.68	0.84	0.88	0.90/0.85
	WSSR ^a	67	37	29	23/34
<i>K. pneumoniae</i> ARC3803	R ²	0.63	0.84	0.91	0.92/0.87
	WSSR ^a	108	50	32	27/42
<i>E. coli</i> ARC3600	R ²	0.72	0.80	0.84	0.77
	WSSR ^a	61	44	37	52
<i>E. coli</i> ARC3805	R ²	0.95	0.98	0.98	0.97
	WSSR ^a	22	12	7.9	15
<i>E. coli</i> ARC3807	R ²	0.60	0.76	0.88	0.87
	WSSR ^a	115	77	39	46

Goodness-of-fit parameters for different critical threshold values for the clinical isolates evaluated in the Hollow Fiber System against Aztreonam-Avibactam (Singh, 2015). Unit used for modeling was mg/L which is equivalent to µg/ml. ^a Weighted sum of squared residuals

Sulbactam PK/PD index & magnitude

The goal of this study is to confirm the Sulbactam PK/PD driver. Sulbactam hollow fiber studies were conducted against susceptible *A. baumannii* strains to confirm its PK/PD efficacy driver. The system was dosed with Sulbactam, every 24hr, every 12hr, every 6hr and mimic a 2hr half-life in the system for 24hr. PK results show (Figure 16) some degradation of Sulbactam in the hollow fiber system, however the degradation was not significant enough that observed data and the predicted data were still within the system limits (Figure 16). Sulbactam degradation could be due to accumulation of β -lactamase in the system, since the fibers act as filters, anything larger than 20 kilo Dalton will not be able to pass through the fibers. Drugs tested in the system are small molecules that can freely pass through the fibers. The same was observed with Aztreonam when dosed alone in the system (Figure 9). However, the degradation was not as profound with Aztreonam compared to Sulbactam. Observed PK data was used throughout, rather than theoretical data were used to determine the PK/PD driver.

PK/PD driver for Sulbactam

Rapid bacterial kill of at least 2 \log_{10} was observed within 4hrs of dosing when sulbactam was dosed once-a-day and multiple times a day against *A. baumannii* ARC2058 in the system (Figure 17). Once a day dosing showed rebound of bacterial culture at 24hrs (Figure 17A). However, dosing the system more frequently showed a better response and suppression of bacterial growth (Figure 17B). PK/PD analysis showed a magnitude of 80%, implying that the Sulbactam concentration needs to be kept above the MIC value for at least 80% of the study duration (24hr) to achieve optimal bacterial kill. One compartment

model using Phoenix 6.2.0 was utilized to determine PK/PD indexes for Sulbactam. Drug exposure was correlated with the changed in bacterial burden at 24hr relative to the starting inoculum at 0hr. Sigmoidal-response (Emax) model was used to analyze the PK/PD index for Sulbactam. Additional exposure parameters such as C_{max} , AUC were analyzed but found weaker correlations (Figure 18). An R^2 value closer to 1 shows a stronger correlation of the observed data against the modeled data. Published data reported a similar PK/PD driver and magnitude for sulbactam against a different *A. baumannii* β -lactam susceptible strain in a similar *in vitro* PK/PD system (Housman, 2013).

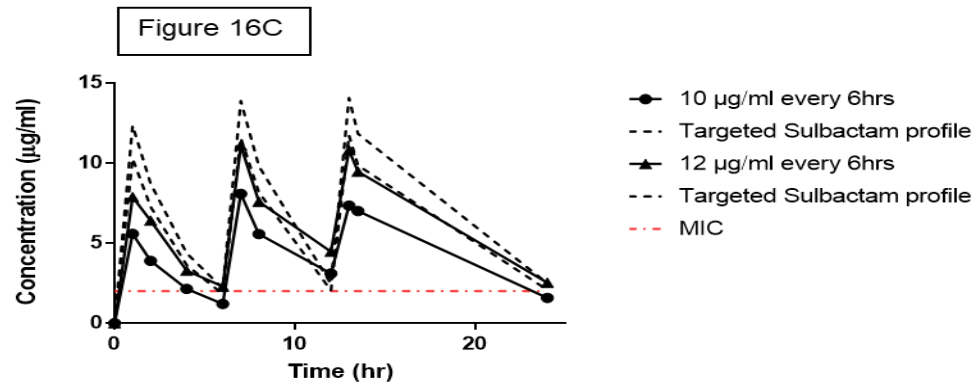
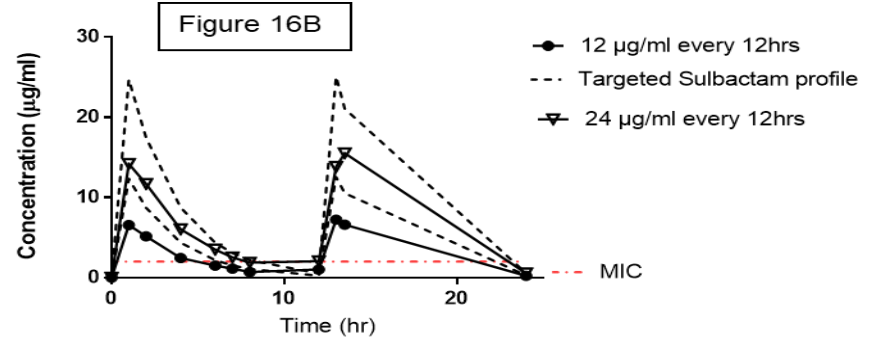
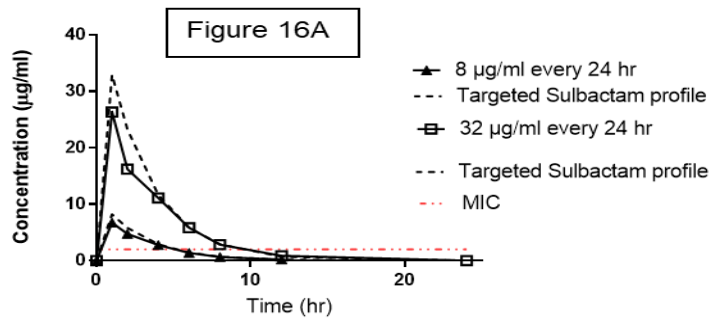


Figure 16: Sulbactam concentration-time profile.

Solid line represent Sulbactam profile observed in the hollow fiber system. Fluctuating dash line represent target Sulbactam profile. Continuous dash line represent the MIC value. Profile represents concentrations in different cartridges infected with a sulbactam susceptible strain of *A. baumannii*, ARC2058. The fourth dose for (q6h) was not sampled. Graphs are labeled based on the targeted C_{max} and regimen.

Figure 17A

Sulbactam 2058 DR

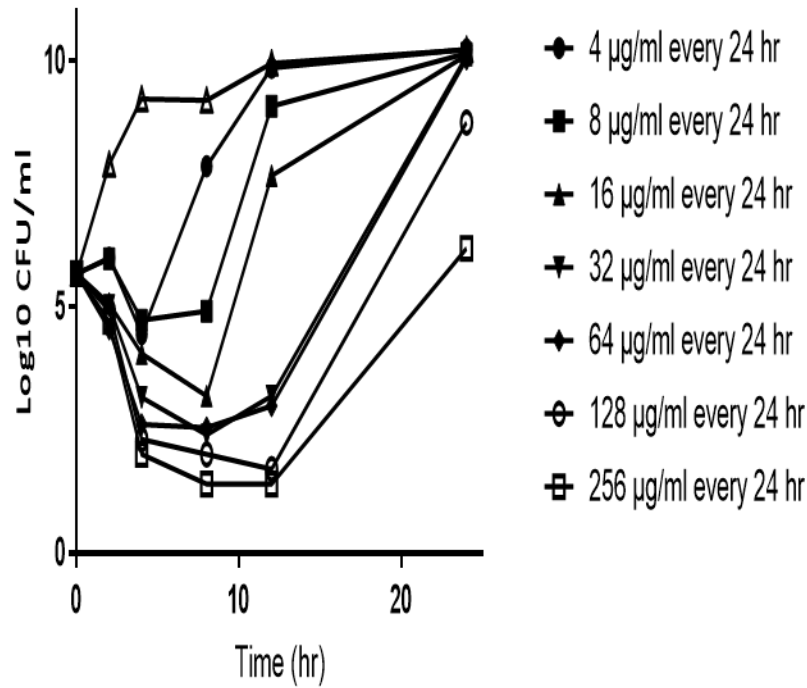


Figure 17B

Sulbactam 2058 DF

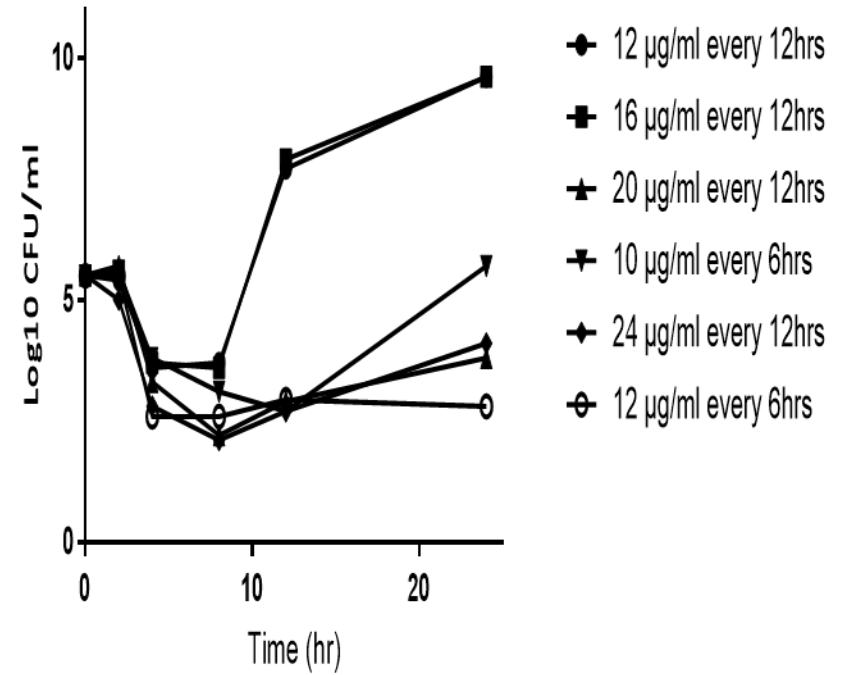
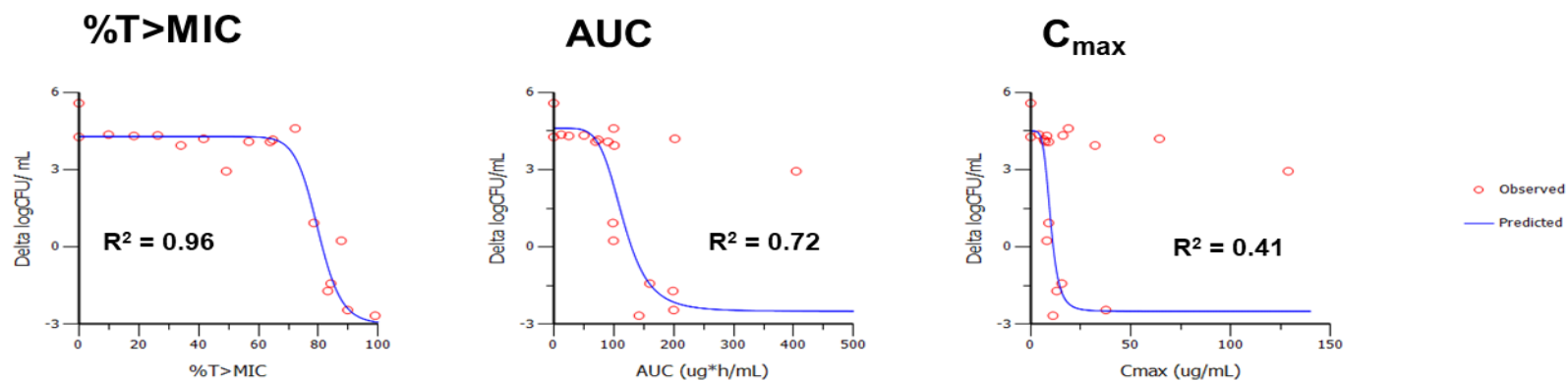


Figure 17: Bacterial response to varying concentrations of Sulbactam against *A. baumannii* ARC2058.

Bacterial response to different Sulbactam dose and regimen. Graphs are labeled based on the targeted C_{max} and regimen.



Secondary parameter for %T>MIC			
Parameter	Estimate	StdError	CV%
STASIS	81.31	1.35	1.67
LOGKILL1	83.78	1.58	1.89
LOGKILL2	87.40	2.40	2.74

Figure 18: Emax model to determine PK/PD relationship for Sulbactam against *A.baumannii*.

Emax model to determine PK/PD relationship comparing AUC/MIC, C_{max}/MIC and %T>MIC for Sulbactam against A. baumannii ARC2508 in the hollow fiber system. Circles represent the observed data while the continuous line represent the predicted best-fit model.

ETX2514 PK/PD index & magnitude

To determine the PK/PD index and magnitude for ETX2514, fixed dose of Sulbactam, which covers 80 %T>MIC of the combination Sulbactam-ETX2514, was ran in the hollow fiber system in combination with varying dose regimen of ETX2514 (Figure 22). Multi-drug resistant *A. baumannii* strains ARC5081 and ARC5079 were utilized for these studies. These strains were chosen based on their Sulbactam-ETX2514 MIC of 2µg/ml and 1µg/ml, respectively, to determine if the combination Sulbactam-ETX2514 can cover bacterial strains with these MIC values, based on the MIC90 of the combination Sulbatam-ETX2514.

In the absence of ETX2514, Sulbactam degradation was observed in the system (Figure 19). Sulbactam hydrolysis was at its lowest when a Sulbactam-susceptible strain was used, which suggests correlation of drug resistance in the presence of β-lactamases. Co-dosing Sulbactam with ETX2514 showed the compound sulbactam concentration in the bacterial compartment of the system was comparable with the compound concentration observed in the central reservoir (Figure 5), indicating the absence of degradation (Figure 16). Similar degradation and protection were observed with Aztreonam alone studies and Avibactam. This demonstrates ETX-2514 and Avibactam's ability of protecting Sulbactam and Aztreonam, respectively, against enzyme hydrolysis.

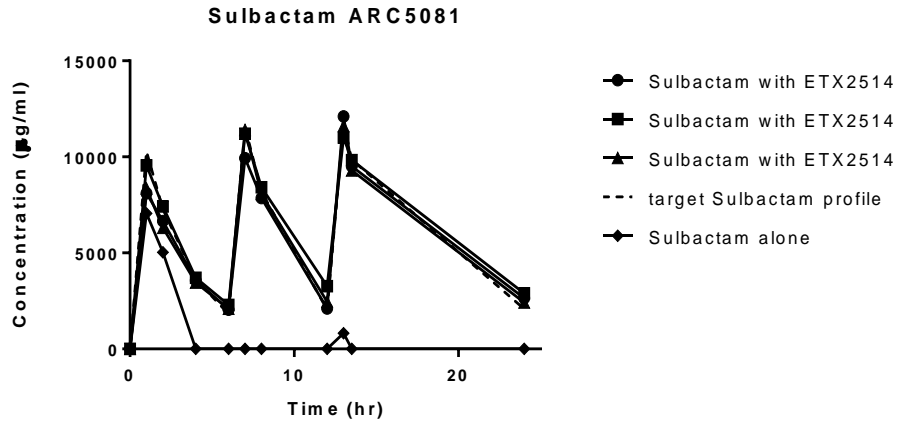


Figure 19: Sulbactam concentration-time profile.

Sulbactam concentration profiles in the Hollow Fiber System in the presence or absence of ETX2514. System was infected with either A. baumannii ARC5801 or ARC5079. Graphs are labeled based on the targeted C_{max} and regimen.

PK/PD driver for ETX2514

Rapid bacterial kill of at least 2 \log_{10} was observed for both ARC5081 and ARC5079 when ETX2514 was dosed with Sulbactam covering 80% of the bacterial MIC for a 24 hr study duration (Figure 22). The addition of a single high dose of ETX2514 showed inefficiency in maintaining bacterial growth suppression, however, when the same total dose was fractionated throughout the study, bacterial response improved (Figure 20 and Figure 21). PD data for *A. baumannii* ARC5079 showed better efficacy compared to ARC5081 response to the combination Sulbactam and ETX2514 (Figure 21). *A. baumannii* ARC5081 has an MIC of 2.0 μ g/ml while *A. baumannii* ARC5079 has an MIC of 1.0 μ g/ml Sulbactam in the presence of 4.0 μ g/ml ETX2514. *A. baumannii* strains with varying MICs were tested in the system to determine whether clinical regimen can sufficiently cover a range of MICs of different *A. baumannii* strains.

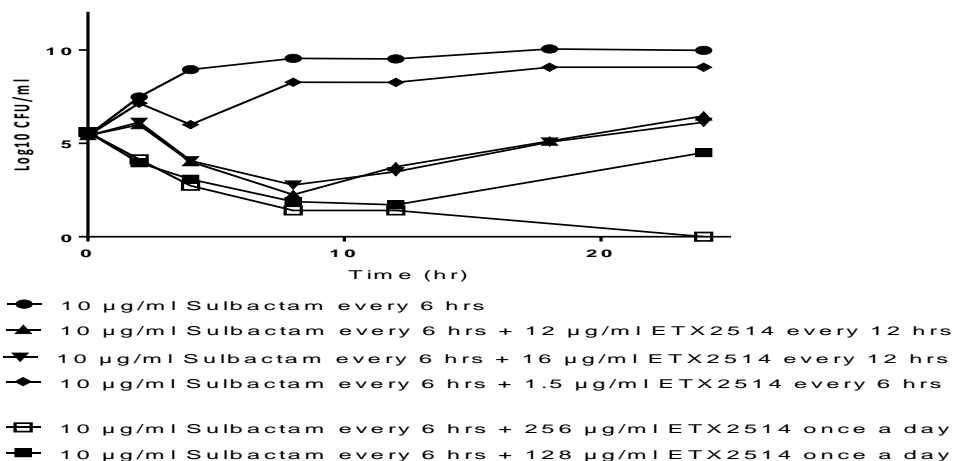


Figure 20: *A. baumannii* ARC5081 response to ETX2514SUL.

Bacterial response to varying concentrations of ETX2514 in the presence of 10µg/ml Sulbactam dosed four times a day against A. baumannii ARC5081. Graphs are labeled based on the targeted C_{max} and regimen.

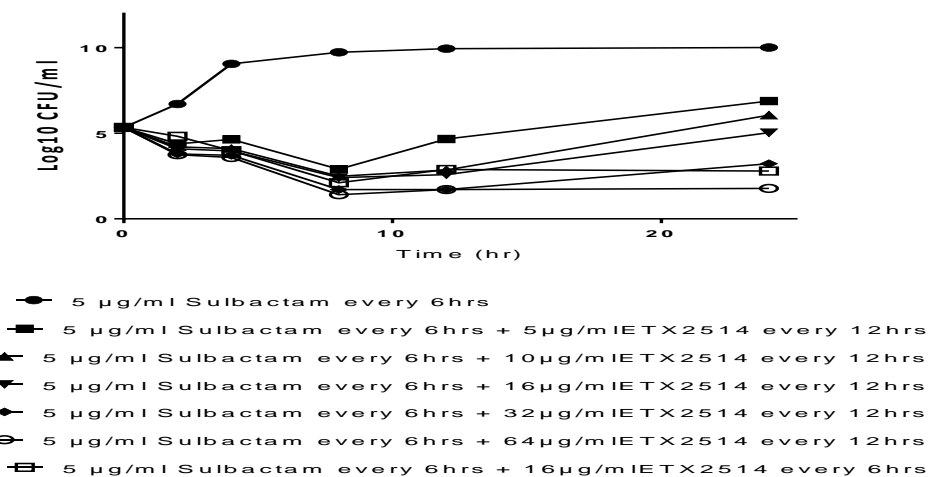


Figure 21: *A. baumannii* ARC5079 response to ETX2514SUL.

Bacterial response to varying concentrations of ETX2514 in the presence of 5µg/ml Sulbactam dosed four times a day against A. baumannii ARC5079. Graphs are labeled based on the targeted C_{max} and regimen.

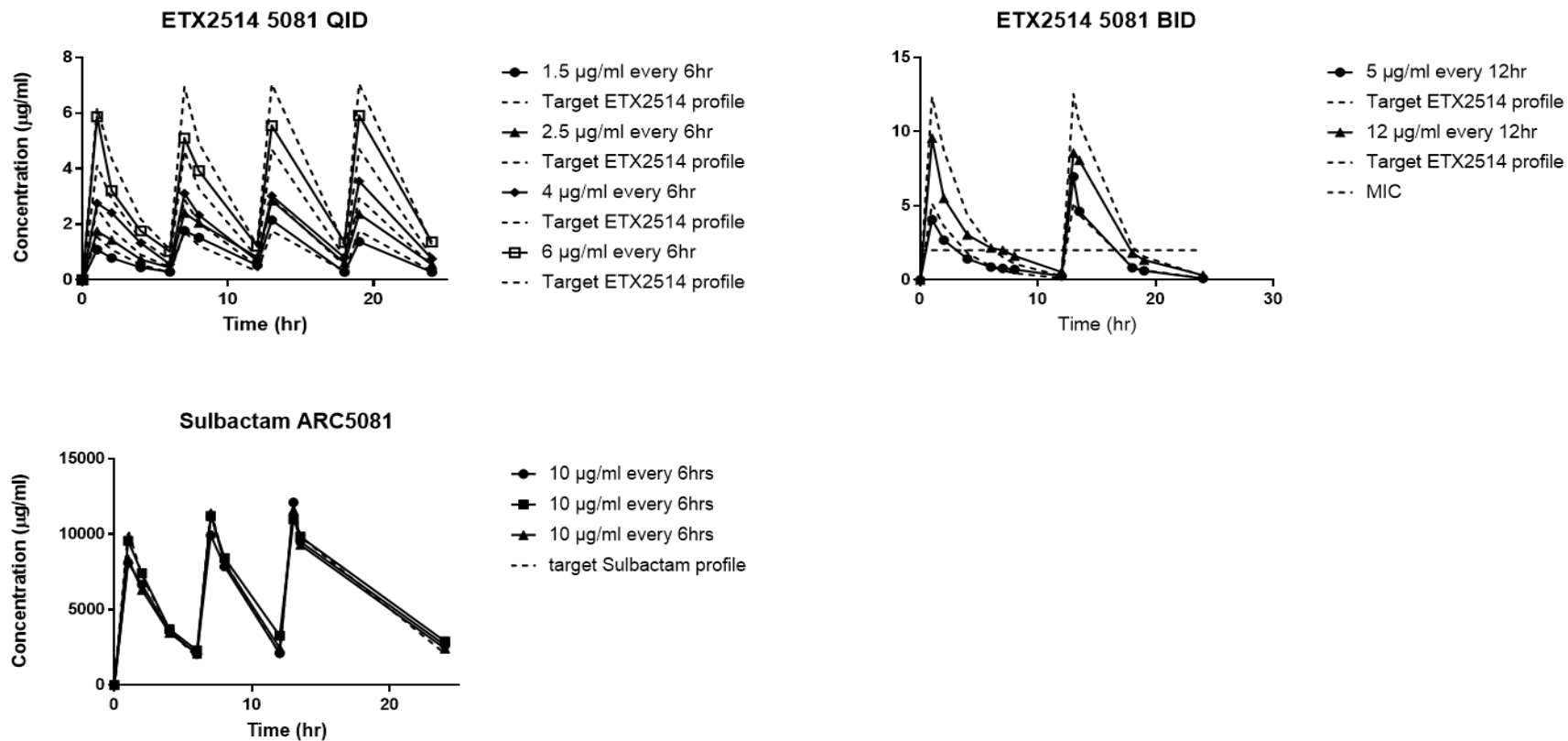


Figure 22: Sulbactam and ETX2514 concentration-time profile.

Representative Sulbactam and ETX2514 concentration profiles in the hollow fiber system. Dash line represent targeted drug profile. System was infected with either *A.baumannii* ARC5081 and ARC5079. Graphs are labeled based on the targeted C_{max} and regimen.

ETX2514 has no intrinsic antibacterial activity against the strains tested in the hollow fiber system. To determine its PK/PD driver, Time above Critical Threshold ($T > C_T$) was applied for this compound. Frequent dosing of ETX2514 in the presence of sulbactam showed better efficacy and suppression of bacterial growth which suggests a time-dependency of the PD effect. Based on the PK/PD for Sulbactam and ETX2514, a range of (1-3 $\mu\text{g/ml}$) critical concentrations were investigated in the hollow fiber system. These are the threshold values utilized to determine the PK/PD index for ETX2514. R^2 (coefficient of correlation) and WSSR (weighted sum of the squared residual) were utilized to determine the goodness of fit of the parameters. These values were determined based on a one compartment model of observed data using Phoenix 6.2.0. Drug exposure was correlated with the changed in bacterial burden at 24hr relative to the starting inoculum at 0hr. Sigmoidal-response model was used to analyze the PK/PD index for ETX2514. $T > C_T$ was highly correlated to efficacy; however, AUC also showed a strong correlation to activity against both strains of *A. baumannii*. Additional exposure parameters such as C_{max} , was analyzed but found no correlation (Figure 23, Table 6). A single PK/PD driver for Sulbactam-ETX2154 was difficult to resolve given the strong correlation for both AUClast and $T > C_T$. AUClast is the area under the drug-time curve from time zero to time of last measurable drug concentration. The magnitude or concentration of drug exposure for the *in vitro* system showed a significantly greater concentration compared to what is needed *in vivo* to achieve efficacy. This disconnect could be associated with the accumulation of β -lactamase in the hollow fiber system. High concentrations of β -lactamases in the system could influence compound integrity which can lead to requiring higher drug exposure for efficacy. This issue is currently being investigated.

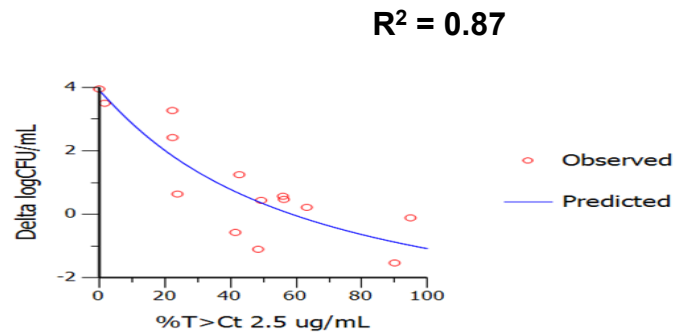
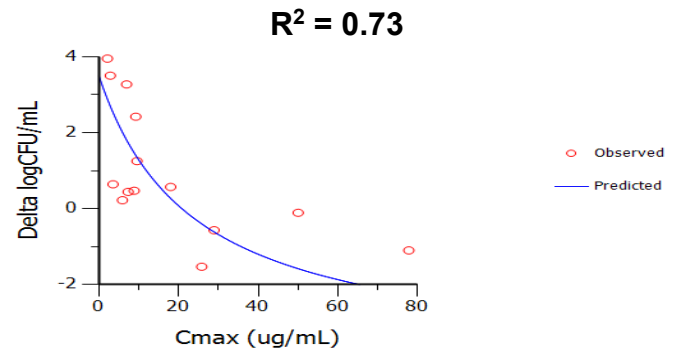
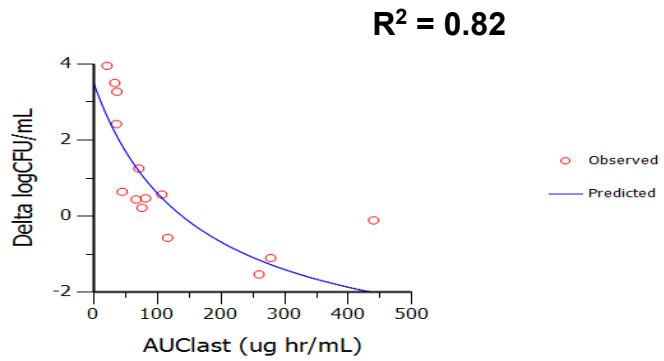


Figure 23: ETX2514 PK/PD E_{max} modeling driver determination for *A. baumannii* ARC5081.

Table 6: Goodness-of-fit parameters for clinical strains against ETX2514Sul.

Clinical isolates	Parameters	AUC	C_{\max}	Critical threshold (C_T) values			
				0.5 mg/L	1 mg/L	2.5 mg/L	4 mg/L
<i>A. baumannii</i> ARC5081	R^2	0.82	0.73	0.37	0.63	0.87	0.81
	WSSR	13	19	33	23	10	14
<i>A. baumannii</i> ARC5079	R^2	0.85	0.83	0.71	0.83	0.87	0.85
	WSSR	38	24	37	24	18	21

Goodness-of-fit parameters for different critical threshold values for the clinical isolates evaluated in the hollow fiber system. Unit used for modeling was mg/L which is equivalent to $\mu\text{g/ml}$.

Chapter IV.

Discussion

Emergence of new mechanisms of antibiotic resistance continually rises and spreads globally, becoming one of the major global health threats. Without new antibiotics being successfully developed, we are getting closer to a post-antibiotic era where a simple cut can become life-threatening.

Significant amounts of time and money are invested on these new drug candidates, however, very few make it to the market, often due to poor PK/PD understanding recognized after the failure of lengthy, expensive clinical testing. The aim of this study is to help assess the use of a dynamic *in vitro* PK/PD system, to help predict successful clinical dose, and PK/PD target and regimen that would help reduce the development of resistance. *In vitro* and *in vivo* PK/PD models have previously been utilized to help characterize potential drug candidates and their PK/PD properties that would help streamline drug development in its early stages or preventing them from entering development in the first place (Meihbom 2002).

In this study, we showed how the dynamic *in vitro* hollow fiber system, can be utilized in combination with *in vivo* PK/PD model to help determine optimal clinical dose and regimen. β -lactam/ β -lactamase inhibitor (BL/BLI) combination faced some challenges in effectively evaluating the PK/PD index and dose regimen (Singh, 2015). Very few studies looked at effective dose combinations that can cover a wide range of clinical isolates. VanScoy et al looked at tazobactam and ceftolozane combination in an *in vitro*

infection model and observed a varied tazobactam threshold value that ranges from 0.5 – 4µg/ml. The authors suggested that dose regimen should be tailored based on the isolates MIC value (VanScoy, 2013). Tailoring each dose for each strain can be challenging in a clinical setting. Data from this study suggest that a single threshold value for the β -lactamase inhibitor can be determined to help predict optimal clinical dose that can cover *K. pneumoniae* and *E. coli* clinical strains with a range of MICs (Singh, 2015). Aztreonam PK/PD index were verified using the hollow fiber system based on published data. *In vivo* and *in vitro* PK/PD models showed good correlation with its predicted PK/PD driver and magnitude for the Avibactam, with the time above critical threshold of 2-2.5µg/ml. Further clinical dose evaluation needs to be assessed to confirm efficacious clinical dose, however, a strong PK/PD correlation between *in vivo* and *in vitro* PK/PD model suggests a strong PK/PD model system effective in predicting optimal clinical dose.

ETX2514Sul is a new BL/BLI combination that would help address serious infections caused by multi-drug resistant strains of *A. baumannii*. This strain of bacteria has been linked to serious infections, such as pneumonia, urinary tract infection, and skin and soft tissue infections etc. ETX2514 is a novel β -lactamase inhibitor that is active against different classes of β -lactamases and can help restore antibacterial property activity of sulbactam against multi-drug resistant strains of *A. baumannii* (Durand, 2017).

In this study, the therapeutic potential of ETX2514Sul was evaluated using the dynamic *in vitro* hollow fiber system. Evaluation of the therapeutic potential of ATM-AVI in the hollow fiber system, was straightforward. Data from this study showed a strong correlation between *in vivo* (murine model) and *in vitro* PK/PD parameters for ATM-AVI. Given this information, the same principle used in determining the PK/PD threshold for

ATM-AVI was applied to ETX2514Sul. Hollow fiber studies utilizing susceptible strains of *A. baumannii* helped confirm the known clinical sulbactam PK/PD index as Time above MIC (Drugs@FDA). Sulbactam resistant strains were utilized in the hollow fiber system to help determine the optimal dose combination for ETX2514Sul. Data suggest a strong correlation of efficacy of ETX2514 with time above critical threshold of 2.5 μ g/ml and a PK/PD index for Sulbactam at 80%-time above MIC, however, data in the hollow fiber system showed that Time above critical threshold and AUC have equally good correlation for efficacy for ETX2514 in the *in vitro* system. Unlike ATM-AVI studies, a single PK/PD driver for ETX2514Sul was not successfully resolved in the hollow fiber system. Data also showed a disconnect between the *in vivo* and *in vitro* PK/PD index and magnitude. *In vitro* data suggest a higher magnitude exposure for Sulbactam is needed for efficacy, 80% time above MIC for Sulbactam while murine PK/PD model data showed efficacy at a much lower magnitude of 20-40% time above MIC. It was hypothesized that this *in vivo/in vitro* disconnect can be attributed to the accumulation of β -lactamase in the hollow fiber system, which is not an issue observed for ATM-AVI hollow fiber studies.

The molecular weight cutoff of the hollow fiber cartridges used in the study, ranged from 5-20 kilo Dalton. Since the hollow fibers act as filters, anything larger than 20 kilo Dalton will not be able to pass through the system. The molecular weight of various β -lactamases is about 50 kilo Dalton which lead to the hypothesis that accumulation of β -lactamases could have an effect in determining the PK/PD index for ETX2514Sul. Accumulation of β -lactamases in the hollow fiber system did not affect the PK/PD data for ATM-AVI. Several leads were pursued to determine why accumulation of β -lactamases in the hollow fiber had a more significant effect on the combination ETX2514Sul and not

ATM-AVI. Concentrations of β -lactamase in both *in vivo* and *in vitro* samples showed higher accumulation of β -lactamases *in vitro*. Different strains also showed difference in β -lactamase accumulation (Data not shown).

The hollow fiber system has several limitations. The system cannot mimic the immune system, the hollow fiber cartridges can be expensive although murine model can be more expensive, and accumulation of bacterial enzyme could have an effect in the outcome of the study.

To address the *in vivo/in vitro* disconnect, a different PK/PD system was utilized (data now shown). Chemostat system utilized the same set-up as the hollow fiber system but without the use of the cartridges (VanScoy, 2013). This dilutes accumulation β -lactamase in the system. Preliminary data from the chemostat system identified %T>MIC as the PK/PD driver, however, with a lower magnitude than that identified with the hollow fiber system, which was more in line with *in vivo* data. The hollow fiber Sulbactam-ETX2514 data suggest a magnitude of 80% T>MIC is needed for Sulbactam to achieve a 1-log kill in the system while data from the chemostat and murine model falls around 50% T>MIC. ETX-2514 show a correlation of efficacy with time above critical threshold of 2.5 μ g/ml in the hollow fiber system while the chemostat system showed 0.75 μ g/ml, which correlates well with *in vivo* murine model data. Both *in vitro* PK/PD model also showed a strong correlation of AUC for efficacy. This suggests that although the hollow fiber system was able to predict the PK/PD driver for ETX2514Sul, forecasting its magnitude was a limitation.

Even with its limitations, the system can be a valuable tool in assessing dose regimen that are biologically and pharmacologically relevant. It can also provide

significant data that can help assess resistance development. The hollow fiber system is a valuable tool in studying drug combination that can be difficult to simulate *in vivo* murine model due to different dosing regimen and half-life that might be difficult to simulate *in vivo* providing an effective tool in assessing PK/PD index in a clinical setting. Even though there is a disconnect with both the hollow fiber data and murine PK/PD model data, both models suggest the same PK/PD driver.

Given the strong correlation of AUC in the hollow fiber system and preliminary data from the Chemostat system, and *in vivo* murine model for the ETX2514 efficacy, clinical dose projections are being modeled around these data set. Achieving a good *in vitro* and *in vivo* correlation translates to a higher confidence in predicting an effective clinical dose. This study was able to show the robust data generated in a dynamic *in vitro* hollow fiber system that can help predict efficacious clinical doses. Assessing an effective clinical dose is one of the many steps in a successful clinical trial. PK/PD target model prediction plays a crucial role in designing an effective clinical dose regimen and the hollow fiber system can help provide useful data for a successful dose prediction.

Appendix A

LC-MS/MS conditions

Column	Atlantis T3, 3 μ , 50 x 3.0mm	
Column Temperature	35 ⁰ C	
Flow rate	1.200 mL/min	
Gradient	Time (min)	%B
	0.50	2
	1.50	98
	2.00	98
	2.01	2
	2.25	Stop
Divert Valve	Time (min)	Position
	0.5	To waste
	2.0	To mass spectrometer
Autosampler Temperature	10 ⁰ C	
Mobile Phase A	Water + 0.1% formic acid	
Mobile Phase B	Acetonitrile + 0.1% formic acid	

MS/MS Parameters (API 5000):

Ion Mode	ESI-	Curtain Gas	45
----------	------	-------------	----

Nebulizer Current or IS Voltage (volt)	-4000	CAD Gas	12
GS1	60	GS2	60
Temperature	600	Injection Volume (µL)	5.0
Q1 Resolution	Unit	Q3 Resolution	Unit

MRM Transitions:

Drug ID	Q1	Q3	DP	CE	CXP
Aztreonam	433.94	95.80	-30	-20	-13
Avibactam	264.10	96	-60	-20	-15
ETX02514-009	276.10	96.1	-40	-27	-15
ETX-010151 (Sulbactam)	232.10	140.0	-40	-25	-15
Carbutamide (IS)	270.00	171.00	-55	-25	-10

Bibliography

- American Chemical Society. (1999). The Discovery and Development of Penicillin. 1928-1945. In *American Chemical Society (ACS)*. Washington, DC.
- Aminov, R. I. (2010). A Brief History of the Antibiotic Era: Lessons Learned and Challenges for the Future. *Frontiers in Microbiology*, 134.
- Blaser, J. (1985). In-vitro model for simultaneous simulation of the serum kinetics of two drugs with different half-lives. *Journal Antimicrobial Chemotherapy*, 15 Suppl A: 125-130.
- Blumenthal, D., & Garrison, J. C. (2011). *Chapter 3: Pharmacodynamics: Molecular Mechanisms of Drug Action*. China: The McGraw-Hill Companies, Inc.
- Bradford, P. A., & Sanders, C. C. (1993). Use of a predictor panel to evaluate susceptibility test methods proposed for piperacillin-tazobactam. *Antimicrobial Agents and Chemotherapy*, 2578-2583.
- Broden, R. N., & Heel, R. C. (1986). Aztreonam. A review of its antibacterial activity, pharmacokinetic properties and therapeutic use. . *Drugs*, 96-130.
- Cadwell, J. J. (2012). The hollow fibre infection model for antimicrobial pharmacodynamics and pharmacokinetics. . *Advances in Pharmacoepidemiology and Drug Safety*, S1:007.
- Centers for Disease Control and Prevention. (2017, August 18). *Antibiotic / Antimicrobial Resistance (AR / AMR)*. Retrieved from www.cdc.gov/drugresistance/index.html

Clinical and Laboratory Standards Institute. (2006). CLSI M07-A7 Methods for dilution antimicrobial susceptibility tests for bacteria that grow aerobically approved standard. *Clinical and Laboratory Standards Institute*, Volume 6. Number 2.

Coates, A. R., Halls, G., & Hu, Y. (2011). Novel Classes of Antibiotics or More of the Same? *British Journal of Pharmacology*, 184-194.

Crandon, J. L., Schuck, V., Banevicius, M., Beaudoin, M., Nichols, W., Tanudra, M., & Nicolau, D. (2012). Comparative in vitro and in vivo efficacies of human simulated doses of ceftazidime and ceftazidime-avibactam against *Pseudomonas aeruginosa*. *Antimicrobial Agents and Chemotherapy*, 6137-6146.

Drusano, G. L. (2004). Antimicrobial pharmacodynamics: Critical interactions of 'bug and drug'. *Nature Reviews Microbiology*, 2:289-300.

Durand-Réville, T., Guler, S., Comita-Prevoir, J., Chen, B., Bifulco, N., Huynh, H., . . . Miller, A. A. (2017). ETX2514 is a broad-spectrum β -lactamase inhibitor for the treatment of drug-resistant Gram-negative bacteria including *Acinetobacter baumannii*. *Nature Microbiology*, 2:17104.

Ehmann, D. E., Jahic, H., Ross, P. L., Gu, R. F., Durand-Réville, T. F., Lahiri, S., . . . Fisher, S. L. (2013). Kinetics of avibactam inhibition against Class A, C, and D β -lactamases. *The Journal of Biological Chemistry*, 27960-27971.

Evans, B. A., & Amyes, S. G. (2014). OXA β -lactamases. *Clinical Microbiology Reviews*, 241-263.

- Infectious Diseases Society of America. (2010). The 10 x '20 Initiative: pursuing a global commitment to develop 10 new antibacterial drugs by 2020. *Clinical Infectious Diseases*, 1081-1083.
- Kong, K.-F., Schneper, L., & Mathee, K. (2010). Beta-lactam Antibiotics: From Antibiosis to Resistance and Bacteriology. *APMIS: Journal of Pathology, Microbiology and Immunology*, 1-36.
- Krans, B. (2014, July 22). *Few New Drugs: Why the Antibiotic Pipeline Is Running Dry*. Retrieved from Healthline: www.healthline.com/health/antibiotics/why-pipeline-running-dry#decline2
- Lahiri, S., Johnstone, M., Ross, P., McLaughlin, R., Olivier, N., & Alm, R. (2014). Avibactam and Class C β -Lactamases: Mechanism of Inhibition, Conservation of the Binding Pocket, and Implications for Resistance. *Antimicrobial Agents and Chemotherapy*, 5704-5713.
- Martínez, J. L. (2012). Natural Antibiotic Resistance and Contamination by Antibiotic Resistance Determinants: The Two Ages in the Evolution of Resistance to Antimicrobials. *Frontiers in Microbiology*, 1.
- McSharry, J. J., Deziel, M. R., Zager, K., Weng, Q., & Drusano, G. L. (2009). Pharmacodynamics of cidofovir for vaccinia virus infection in an in vitro hollow-fiber infection model system. *Antimicrobial Agents and Chemotherapy*, 129-135.
- Meibohm, B., & Derendorf, H. (2002). Pharmacokinetic/pharmacodynamic studies in drug product development. . *Journal of Pharmaceutical Sciences*, 18-31.

- Munita, J. M., & Arias, C. A. (2016). Mechanisms of Antibiotic Resistance. *Microbiology Spectrum*, 2.
- Nielsen, E. I., & Friberg, L. E. (2013). Pharmacokinetic-pharmacodynamic modeling of antibacterial drugs. *Pharmacological Reviews*, 1053-1090.
- Oberoi, L., Singh, N., Sharma, P., & Aggarwal, A. (2013). ESBL, MBL and Ampc β Lactamases Producing Superbugs – Havoc in the Intensive Care Units of Punjab India. *Journal of Clinical & Diagnostic Research*, 70-73.
- Paterson, D. L., & Bonomo, R. A. (2005). Extended-Spectrum β -Lactamases: a Clinical Update. *Clinical Microbiology Reviews*, 657-686.
- Paterson, D. L., & Bonomo, R. A. (2005). Extended-Spectrum β -lactamases: a Clinical Update. *Clinical Microbiology Reviews*, 657-686.
- Riccobene, T. A., Su, S. F., & Rank, D. (2013). Single- and multiple-dose study to determine the safety, tolerability, and pharmacokinetics of ceftaroline fosamil in combination with avibactam in healthy subjects. *Antimicrobial Agents and Chemotherapy*, 1496-1504.
- Shaikh, S., Fatima, J., Shakil, S., Rizvi, S. M., & Kamal, M. A. (2015). Antibiotic resistance and extended spectrum beta-lactamases: Types, epidemiology and treatment. *Saudi Journal of Biological Sciences*, 90-101.
- Singh, R., Kim, A., Tanudra, M. A., Harris, J. J., McLaughlin, R. E., Patey, S., . . . Eakin, A. E. (2016). Pharmacokinetics/pharmacodynamics of a β -lactam and β -lactamase

inhibitor combination: a novel approach for aztreonam/avibactam. *The Journal of Antimicrobial Chemotherapy*, 2618-2626.

Stachyra, T., Levasseur, P., Péchereau, M.-C., Girard, A.-M., Claudon, M., Miossec, C., & Black, M. T. (2009). In vitro activity of the β -lactamase inhibitor NXL104 against KPC-2 carbapenemase and Enterobacteriaceae expressing KPC carbapenemases. *Journal of Antimicrobial Chemotherapy*, 326-329.

Stachyra, T., Péchereau, M.-C., Bruneau, J.-M., Claudon, M., Frère, J.-M., Miossec, C., . . . Black, M. T. (2010). Mechanistic Studies of the Inactivation of TEM-1 and P99 by NXL104, a Novel Non- β -Lactam β -Lactamase Inhibitor. *Antimicrobial Agents and Chemotherapy*, 5132-5138.

Struelens, M. J. (1998). The epidemiology of antimicrobial resistance in hospital acquired infections: problems and possible solutions. *British Medical Journal*, 652-654.

US Food and Drug Administration. (n.d.). *Drugs@FDA: FDA Approved Drug Products*. Retrieved from <https://www.accessdata.fda.gov/scripts/cder/daf/>

VanScoy, B., Mendes, R. E., Nicasio, A. M., Castanheira, M., Bulik, C. C., Okusanya, O., . . . Ambrose, P. G. (2013). Pharmacokinetics-pharmacodynamics of tazobactam in combination with ceftolozane in an in vitro infection model. *Antimicrobial Agents and Chemotherapy*, 2809-2814.

Velkov, T., Bergen, P., Lora-Tamayo, J., Landersdorfer, C. B., & Li, J. (2014). PK/PD models in antibacterial development. *Current Opinion in Microbiology*, 5.

World Health Organization (WHO). (2017, November). *Antibiotic resistance*. Retrieved from <https://www.who.int/news-room/fact-sheets/detail/antibiotic-resistance>

Yan, X., & Krzyzanski, W. (2012). Dose correction for the Michaelis–Menten approximation of the target-mediated drug disposition model. *Journal of pharmacokinetics and pharmacodynamics*, 141-146.